

## Exclusive nonleptonic $B_c$ -meson decays to $S$ -wave charmonium states

Lopamudra Nayak<sup>1,\*</sup>, P. C. Dash<sup>1</sup>, Susmita Kar<sup>2</sup>, and N. Barik<sup>3</sup>

<sup>1</sup>*Department of Physics, Siksha 'O' Anusandhan (Deemed to be University), Bhubaneswar 751030, India*

<sup>2</sup>*Department of Physics, Maharaja Sriram Chandra Bhanja Deo University, Baripada 757003, India*

<sup>3</sup>*Department of Physics, Utkal University, Bhubaneswar 751004, India*



(Received 29 December 2021; accepted 18 February 2022; published 22 March 2022)

We study the exclusive two-body nonleptonic  $B_c \rightarrow X_{c\bar{c}}M$  decays, where  $X_{c\bar{c}}$  is either a ground ( $1S$ ) or a radially excited ( $2S$  or  $3S$ ) charmonium, and  $M$  is a pseudoscalar ( $P$ ) or a vector ( $V$ ) meson. We consider here three categories of decays:  $B_c \rightarrow PP, PV, VP$  decays within the framework of a relativistic independent quark (RIQ) model based on a flavor-independent interaction potential in scalar-vector harmonic form. Using the factorization approximation, we calculate the weak form factors from the overlapping integrals of meson wave functions obtained in the RIQ model and predict the branching fractions for a set of exclusive nonleptonic  $B_c$  decays in reasonable agreement with other model predictions. Some of the decays of interest are found to have branching fractions  $\sim(10^{-3} - 10^{-4})$  within the detection ability of the current experiments and can be precisely measured at LHCb in the near future. In the wake of the recent measurement of  $B_c \rightarrow J/\psi\pi(K)$ ,  $B_c \rightarrow J/\psi\pi(D_s)$ ,  $B_c \rightarrow \pi(J/\psi, \psi(2S))$ , and  $B_c \rightarrow J/\psi(\pi, \mu\nu)$  reported by the LHCb and ATLAS Collaborations, we predict the ratios  $\mathcal{R}_{K/\pi}$ ,  $\mathcal{R}_{D_s/\pi}$  and  $\mathcal{R}_{\psi(2S)/J/\psi}$  in broad agreement with the data from LHCb and ATLAS Collaborations. Our predicted ratio  $\mathcal{R}_{\pi/\mu\nu}$  is found to be underestimated. The results indicate that the present approach works well in the description of exclusive nonleptonic  $B_c$  decays within the framework of the RIQ model.

DOI: [10.1103/PhysRevD.105.053007](https://doi.org/10.1103/PhysRevD.105.053007)

### I. INTRODUCTION

The  $B_c$  meson is unique because of its two outstanding characteristics features: (1) It is the lowest bound state of two heavy quarks with open (explicit) flavor quantum numbers: a bottom quark (antiquark) and a charm antiquark (quark). The other heavy quark in the Standard Model, i.e., the top quark, cannot form a hadron because of it has too short of a lifetime to be hadronized. (2) It can decay only via weak interactions, since pure strong and electromagnetic interacting processes conserve flavors. Being a ground state of a  $(b\bar{c})$  system, it lies below the  $BD$  meson decay threshold, with either of its constituent quarks being heavy which can decay individually, and very rich  $B_c$ -decay channels are expected with sizable branching ratios and comparatively long lifetimes [1]. This makes  $B_c$  meson an ideal system for studying heavy quark dynamics.

Ever since the discovery of a  $B_c$  meson at Fermilab by the CDF Collaboration [2] two decades ago, a lot of

experimental probes have happened in this sector yielding detection of many ground and excited heavy meson states including the radially excited states  $\psi(2S)$  and  $\eta_c(2S)$  [3]. Many new  $B_c$ -decay channels have also been observed by the LHCb Collaboration [4–8]. The high luminosity available at LHC makes it possible to measure various decay channels including those into charmonium states [9–11]. Around  $\mathcal{O}(10^9)$ ,  $B_c$  events with a cross section of  $1 \mu\text{b}$  and luminosity of  $1 \text{ fb}^{-1}$  [12] expected at the LHCb are likely to provide sufficient data for a systematic study of the  $B_c$  family. Among many observations on  $B_c$  decays in recent times, the decay  $B_c \rightarrow J/\psi K$  is observed for the first time by the LHCb Collaboration, and the measurement of ratios of branching fractions  $\mathcal{R}_{K/\pi}$  [13,14] are found to be

$$\begin{aligned} \mathcal{R}_{K/\pi} &= \frac{\mathcal{B}(B_c \rightarrow J/\psi K)}{\mathcal{B}(B_c \rightarrow J/\psi\pi)} \\ &= \begin{cases} 0.069 \pm 0.019(\text{stat.}) \pm 0.005(\text{syst.}) \\ 0.079 \pm 0.007(\text{stat.}) \pm 0.003(\text{syst.}) \end{cases} \end{aligned}$$

The ratios of branching fractions  $\mathcal{R}_{D_s/\pi}$  [6,15],  $\mathcal{R}_{\psi(2S)/J/\psi}$  [16] observed by LHCb collaboration are

$$\mathcal{R}_{D_s/\pi} = \frac{\mathcal{B}(B_c \rightarrow J/\psi D_s)}{\mathcal{B}(B_c \rightarrow J/\psi\pi)} = \begin{cases} 2.9 \pm 0.57 \pm 0.24 \\ 3.8 \pm 1.1 \pm 0.4 \pm 0.2 \end{cases},$$

\*lopalmn95@gmail.com

Published by the American Physical Society under the terms of the [Creative Commons Attribution 4.0 International license](https://creativecommons.org/licenses/by/4.0/). Further distribution of this work must maintain attribution to the author(s) and the published article's title, journal citation, and DOI. Funded by SCOAP<sup>3</sup>.

$$\mathcal{R}_{\psi(2S)/J/\psi} = \frac{\mathcal{B}(B_c \rightarrow \psi(2S)\pi)}{\mathcal{B}(B_c \rightarrow J/\psi\pi)} = 0.250 \pm 0.068(\text{Stat.}) \\ \pm 0.014(\text{Syst.}) \pm 0.006,$$

where the last correction term accounts for the uncertainty of  $\frac{\mathcal{B}(\psi(2S) \rightarrow \mu^+\mu^-)}{\mathcal{B}(J/\psi \rightarrow \mu^+\mu^-)}$ . The first measurement of the ratio  $\mathcal{R}_{\pi^+/\mu^+\nu}$  [17] relating the nonleptonic and semileptonic  $B_c$ -decay rates is also performed by the LHCb Collaboration yielding

$$\mathcal{R}_{\pi^+/\mu^+\nu} = \frac{\mathcal{B}(B_c \rightarrow J/\psi\pi)}{\mathcal{B}(B_c \rightarrow J/\psi\mu^+\nu)} = 0.049 \pm 0.0028(\text{Stat.}) \\ \pm 0.0046(\text{Syst.}),$$

which is found at the lower end of the available theoretical predictions.

The detection of ground and excited charmonium states and measured observables in the nonleptonic and semileptonic  $B_c$  decays to charmonium ground and excited states are of special interest as it is easier to identify them in the experiment. The two-body nonleptonic  $B_c$  decays have been widely studied using various theoretical approaches and phenomenological models (see the classified bibliography of Ref. [18]). Most of these studies deals with the  $B_c$ -meson decay to daughter mesons in their ground states only. Among several theoretical studies on nonleptonic  $B_c$ -meson decays to radially excited charmonium and charm meson states, the perturbative QCD approach based on  $k_T$  factorization [19–21], light front quark model using modified harmonic oscillator wave functions [22], ISGW2 quark model [23], relativistic constituent quark model [24], relativistic constituent quark model based on Bethe-Salpeter formalism [25], improved instantaneous approximation of the original Bethe-Salpeter equation and Mandelstam approach [26], perturbative QCD approach [27], relativistic instantaneous approximation of the original Bethe-Salpeter equation [28], quark model based on improved Bethe-Salpeter approach [29,30], nonrelativistic constituent quark model [31], relativistic constituent quark model [32], relativistic quark model [33], QCD factorization using BSW model and light front quark model [34], QCD relativistic quark potential model [35], covariant confined quark model [36,37] and the relativistic constituent quark model [38] are noteworthy. In their recent analysis [20], Rui *et al.* predicted the ratio between the decay modes  $B_c \rightarrow \psi(2S)\pi$  and  $B_c \rightarrow J/\psi\pi$  in comparison with experimental data within uncertainties and the branching fraction of  $B_c \rightarrow \eta_c(2S)\pi \sim 10^{-3}$  that can hopefully be measured in the LHCb experiment. The recent predictions [29,30] of Zhou and co-workers on the branching fractions of radially excited  $2S$  and  $3S$  charmonium states  $\sim 10^{-4}$  lie within the detection accuracy of current experiments. The detection of such decays to radially excited charmonium states, observed ratios of branching fractions, and recent

predictions of branching fractions in this sector by different model approaches provide us necessary motivation to study these noneptonic  $B_c$  decays within the framework of our relativistic independent quark (RIQ) model.

The RIQ model, developed by our group, has been applied in a wide-ranging hadronic sector describing the static properties of hadrons [39] and their decay properties in the radiative, weak radiative, rare radiative [40]; leptonic, weak leptonic, radiative leptonic [41]; and semileptonic [42] decays of mesons. In our recent analysis, we predict the magnetic dipole and electromagnetic transitions of  $B_c$  and  $B_c^*$  mesons in their ground as well as excited states [43]; the exclusive semileptonic  $B_c$ -meson decays to the charmonium ground states in the vanishing [44] and non-vanishing [45] lepton mass limit. In this model, our group has predicted [46,47] the exclusive two-body nonleptonic decays of heavy flavored mesons to the charmonium and charm mesons in their ground states. We would like to extend the application of the RIQ model to analyze two-body nonleptonic  $B_c$  decays to the  $S$ -wave charmonium states ( $nS$ ) along with a light or charm meson state, where  $n = 1, 2, 3$ , and provide a ready reference to existing and forthcoming experiments. We ignore the decay channels involving higher  $4S$  charmonia, since their properties are still not understood well.

The description of nonleptonic decay is notoriously nontrivial as it is strongly influenced by confining color forces, and it involves matrix elements of local four-quark operators in the nonperturbative QCD approach, the mechanism of which is not yet understood well in the Standard Model framework. If one ignores the weak annihilation contribution, the nonleptonic transition amplitudes are conveniently described in the so-called naive factorization approximation [24,33,35,46–50], which works reasonably well in two-body nonleptonic  $B_c$  decays, where the quark-gluon sea is suppressed in the heavy quarkonium [34]. Bjorken's intuitive argument on color transparency in his pioneering work [51], theoretical development based on the QCD approach in the  $\frac{1}{N_c}$  limit [52], and heavy quark effective theory (HQET) [53] provide justification for such approximation. In the present study, we consider the contribution of the current-current operators [54] only in calculating the tree-level diagram expected to be dominant in these decays. The contribution of the penguin diagram may be significant in the evaluation of a  $CP$  violation and search for new physics beyond the Standard Model. But its contribution to the decay amplitudes in the present analysis is considered less significant. In fact, the QCD and electroweak penguin operators' contribution have been shown [55,56] to be negligible compared to that of current-current operators in these decays due to serious suppression of Cabibbo-Kobayashi-Maskawa (CKM) elements. The Wilson's coefficients of penguin operators being very small, its contribution to the weak decay amplitude is only relevant in

rare decays, where the tree-level contribution is either strongly CKM suppressed as in  $\bar{B} \rightarrow \bar{K}^* \pi$  or matrix elements of current-current operators do not contribute at all as in  $\bar{B} \rightarrow \bar{K}^* \gamma$  and  $\bar{B}^0 \rightarrow \bar{K}^0 \phi$  [54].

The rest of the paper is organized as follows. In Sec. II, we introduce the effective Hamiltonian and factorization for two-body nonleptonic  $B_c$ -meson decay modes induced by  $b \rightarrow c \bar{q}_i q_j$  transition at the quark level. The weak decay form factors representing the hadronic amplitudes, calculated from the overlap integral of meson wave functions in the framework of the RIQ model are described in Sec. III. Section IV is devoted to the numerical results and discussion, and Sec. V contains our brief summary and conclusion. A brief review of the RIQ model framework, wave packet representation of the meson state, and momentum probability amplitudes of the constituent quarks inside the meson bound state are presented in the Appendix.

## II. EFFECTIVE HAMILTONIAN AND FACTORIZATION APPROXIMATION

In this section, we introduce the effective Hamiltonian for two-body nonleptonic  $B_c$  decays induced by  $b \rightarrow c \bar{q}_i q_j$  at the quark level, where  $q_i = u, c$  and  $q_j = d, s$ . As described above, we consider only the contribution of current-current operators at the tree level. Neglecting the contribution of penguin diagrams, the decay modes symbolized by  $B_c \rightarrow X_{c\bar{c}}(nS)M$ , where  $X_{c\bar{c}}$  is the ground and excited charmonium states with  $n = 1, 2, 3$  and  $M$  is a pseudoscalar ( $P$ ) or a vector ( $V$ ) meson, are governed by the effective Hamiltonian [23,24,27,31,38],

$$H_{\text{eff}} = \frac{G_F}{\sqrt{2}} \{ V_{cb} V_{ud}^* [c_1(\mu)(\bar{c}b)(\bar{d}u) + c_2(\mu)(\bar{d}b)(\bar{c}u)] \\ + V_{cb} V_{cs}^* [c_1(\mu)(\bar{c}b)(\bar{s}c) + c_2(\mu)(\bar{s}b)(\bar{c}c)] \\ + V_{cb} V_{us}^* [c_1(\mu)(\bar{c}b)(\bar{s}u) + c_2(\mu)(\bar{s}b)(\bar{c}u)] \\ + V_{cb} V_{cd}^* [c_1(\mu)(\bar{c}b)(\bar{d}c) + c_2(\mu)(\bar{d}b)(\bar{c}c)] \} + \text{H.c.}, \quad (1)$$

where  $G_F$  is the Fermi Coupling constant,  $V_{ij}$  are CKM factors,  $(\bar{q}_\alpha q_\beta)$  is a short notation for  $V-A$  current  $q_\alpha \gamma^\mu (1 - \gamma_5) q_\beta$ , and  $c_{1,2}$  are the Wilson coefficients. With the effective Hamiltonian in the form (1), the decay amplitude for  $B_c \rightarrow X_{c\bar{c}}(nS)M$  is given by

$$A(B_c \rightarrow X_{c\bar{c}}(nS)M) = \langle X_{c\bar{c}}(nS)M | H_{\text{eff}} | B_c \rangle \\ = \frac{G_F}{\sqrt{2}} \sum_i \lambda_i C_i(\mu) \langle \mathcal{O} \rangle_i, \quad (2)$$

where  $\lambda_i$  is the CKM factor, and  $\langle \mathcal{O} \rangle_i$  is the matrix element of the local four-quark operators. In the framework of naive factorization, the nonleptonic decay amplitude is approximated by the product of two matrix elements of quark currents as

$$\langle X_{c\bar{c}}(nS)M | \mathcal{O} | B_c \rangle_i = \langle M | J^\mu | 0 \rangle \langle X_{c\bar{c}}(nS) | J_\mu | B_c \rangle \\ + \langle X_{c\bar{c}}(nS) \leftrightarrow M \rangle, \quad (3)$$

where  $J_\mu$  is the weak current. One of these is the matrix element for the  $B_c$  transition to one final mesons state, while the other matrix element corresponds to the transition from the vacuum to other final meson state. The latter is given by the corresponding meson decay constant. In this way, the hadronic matrix element of four-quark operators can be expressed as the product of the decay constant and invariant weak form factors [23,31,46,47,50,57,58].

Of course, there is difficulty inherent in such an approach because the Wilson's coefficients, which include the short-difference QCD effect between  $\mu = m_N$  and  $\mu = m_b$  are  $\mu$  scale and renormalization scheme dependent, while  $\langle \mathcal{O} \rangle_i$  are  $\mu$  scale and renormalization scheme independent. As a result, the physical amplitude depends on the  $\mu$  scale. However, the naive factorization disentangles the long-distance effects from the short-distance sector assuming that the matrix element  $\langle \mathcal{O} \rangle$  at the  $\mu$  scale contains non-factorizable contributions in order to cancel the  $\mu$  dependence and scheme dependence of  $c_i(\mu)$ ; i.e., the approximation neglects possible QCD interaction between the meson  $M$  and the  $B_c X_{c\bar{c}}$  system [50,58]. In general, it works in some two-body nonleptonic decays of heavy mesons in the limit of a large number colors. It is expected that the factorization scheme works reasonably well in two-body nonleptonic  $B_c$  decays with radially excited charmonium mesons in the final states, where the quark-gluon sea is suppressed in the heavy quarkonium [23,34].

We also neglect here the so-called  $W$  exchange and annihilation diagram, since in the limit  $M_W \rightarrow \infty$  they are connected by Fiertz transformation and are doubly suppressed by the kinematic factor of the order  $(\frac{m_i^2}{M_W^2})$ . We also discard the color octet current which emerges after the Fiertz transformation of color-singlet operators. Clearly, these currents violate factorization since they cannot provide transitions to the vacuum states. Taking into account the Fiertz reordered contribution, the relevant coefficients are not  $c_1(\mu)$  and  $c_2(\mu)$  but the combination

$$a_{1,2}(\mu) = c_{1,2}(\mu) + \frac{1}{N_c} c_{2,1}(\mu). \quad (4)$$

Assuming a large  $N_c$  limit to fix the QCD coefficients  $a_1 \approx c_1$  and  $a_2 \approx c_2$  at  $\mu \approx m_b^2$ , nonleptonic decays of heavy mesons have been analyzed in Refs. [23,27,35,59].

The matrix elements corresponding to the transition from vacuum to one of the final state pseudoscalar ( $P$ ) or vector ( $V$ ) meson are covariantly expanded in terms of the meson decay constant  $f_{P,V}$  as

$$\langle P | \bar{q}'_i \gamma^\mu \gamma_5 q_j | 0 \rangle = i f_P p_P^\mu, \\ \langle V | \bar{q}'_i \gamma^\mu q_j | 0 \rangle = e^{*\mu} f_V m_V. \quad (5)$$

The covariant decomposition of matrix elements of the weak current  $J_\mu$  between initial and final pseudoscalar meson state is

$$\begin{aligned} & \langle P(p_P) | \bar{q}_c \gamma_\mu q_b | B_c(P) \rangle \\ &= \left[ (p + p_P)_\mu - \frac{M^2 - m_P^2}{q^2} q_\mu \right] F_1(q^2) + \frac{M^2 - m_P^2}{q^2} q_\mu F_0(q^2) \\ &= (p + p_P)_\mu f_+(q^2) + (p - p_P)_\mu f_-(q^2), \end{aligned} \quad (6)$$

where

$$f_+(q^2) = F_1(q^2), \quad (7)$$

$$f_-(q^2) = \frac{M^2 - m_P^2}{q^2} [F_0(q^2) - F_1(q^2)]. \quad (8)$$

For transition to the vector meson final state, a corresponding matrix element is parametrized as

$$\langle V(p_V) | \bar{q}_c \gamma_\mu q_b | B_c(p) \rangle = \frac{2V(q^2)}{M + m_V} i \epsilon_{\mu\nu\rho\sigma} e^{*\nu} p^\rho p_V^\sigma \quad (9)$$

and

$$\begin{aligned} & \langle V(p_V) | \bar{q}_c \gamma_\mu \gamma_5 q_b | B_c(p) \rangle \\ &= (M + m_V) e_\mu^* A_1(q^2) - \frac{A_2(q^2)}{M + m_V} (e^* \cdot q) (p + p_V)_\mu \\ & \quad - 2m_V \frac{e^* \cdot q}{q^2} q_\mu A_3(q^2) + 2m_V \frac{e^* \cdot q}{q^2} q_\mu A_0(q^2), \end{aligned} \quad (10)$$

where

$$A_3(q^2) = \frac{M + m_V}{2m_V} A_1(q^2) - \frac{M - m_V}{2m_V} A_2(q^2). \quad (11)$$

Here,  $p, p_{P,V}$  stand for the four momentum of the initial and final state mesons, respectively.  $M$  is the mass of the decaying  $B_c$ , and  $m_P$  and  $m_V$  stand for the mass of the pseudoscalar and vector mesons, respectively, in the final state.  $q = p - p_{P,V}$  denotes the four momentum transfer and  $\hat{e}^*$  the polarization of the final state vector meson. In order to cancel the poles at  $q^2 = 0$ , invariant weak form factors  $F_0(q^2), F_1(q^2), A_0(q^2)$  and  $A_3(q^2)$  satisfy following conditions:

$$F_0(0) = F_1(0) \quad \text{and} \quad A_0(0) = A_3(0).$$

The decay rate for nonleptonic transition  $M \rightarrow P_1 P_2$  is expressed in terms of the decay amplitude  $A(B_c \rightarrow P_1 P_2)$  as

$$\Gamma(B_c \rightarrow P_1 P_2) = \frac{|\vec{k}|}{8\pi M^2} |A(B_c \rightarrow P_1 P_2)|^2, \quad (12)$$

where  $\vec{k}$  is the magnitude of three momentum of the final state meson. In the parent meson rest frame, it is given by

$$\begin{aligned} |\vec{k}| &= |\vec{p}_{P_1}| = |\vec{p}_{P_2}| = \frac{1}{2M} \{ [M^2 - (m_{P_1} + m_{P_2})^2] \\ & \quad \times [M^2 - (m_{P_1} - m_{P_2})^2] \}^{1/2}. \end{aligned} \quad (13)$$

The corresponding expression of the decay rate for  $M \rightarrow PV(VP)$  is obtained in the form

$$\Gamma(B_c \rightarrow PV, VP) = \frac{|\vec{k}|^3}{8\pi m_V^2} |A(B_c \rightarrow PV, VP)|^2, \quad (14)$$

with

$$\begin{aligned} |\vec{k}| &= \frac{1}{2M} \{ [M^2 - (m_{P,V} + m_{V,P})^2] \\ & \quad \times [M^2 - (m_{P,V} - m_{V,P})^2] \}^{1/2}. \end{aligned} \quad (15)$$

The relevant decay amplitude (2) is then expressed in the form

$$\begin{aligned} A &= \frac{G_F}{\sqrt{2}} (\text{CKM factor})(\text{QCD factor})(M^2 - m_{P_1}^2) \\ & \quad \times f_{P_2} F_0^{B_c \rightarrow P_1}(q^2), \\ A &= \frac{G_F}{\sqrt{2}} (\text{CKM factor})(\text{QCD factor}) 2m_V f_V F_1^{B_c \rightarrow P}(q^2), \\ & \quad \text{and} \\ A &= \frac{G_F}{\sqrt{2}} (\text{CKM factor})(\text{QCD factor}) 2m_V f_P A_0^{B_c \rightarrow V}(q^2), \end{aligned}$$

for  $B_c \rightarrow P_1 P_2$ ,  $B_c \rightarrow PV$ , and  $M \rightarrow VP$  decays, respectively. The factorized amplitudes (3) are expressed in terms of meson decay constants ( $f_{P,V}$ ) and weak form factors  $F_0^{B_c \rightarrow P_1}$ ,  $F_1^{B_c \rightarrow P}$ ,  $A_0^{B_c \rightarrow V}$ ; it is straightforward to predict the decay rate for different decay processes in the RIQ model framework.

### III. TRANSITION AMPLITUDE AND WEAK DECAY FORM FACTORS IN THE RELATIVISTIC INDEPENDENT QUARK MODEL

We study two-body nonleptonic  $B_c$  decays in three categories:  $B_c \rightarrow PP$ ,  $B_c \rightarrow PV$  and  $B_c \rightarrow VP$ , where  $P$  and  $V$  stand for pseudoscalar and vector meson final states, respectively. The decay amplitude is calculated here from the relevant tree-level diagram as shown in Fig. 1. The color-favored ‘‘class I’’ decays, represented by Fig. 1(a), are characterized by an external  $W$  emission, where the decay amplitude is proportional to the QCD factor  $a_1(\mu)$ . However the ‘‘class III’’ type decays, represented in Fig. 1(c), are those in which both the QCD factors  $a_1(\mu)$  and  $a_2(\mu)$  interfere, providing effective contribution to the factorized decay amplitude. As described above, we consider the two-body nonleptonic  $B_c$  decays induced by the  $b \rightarrow c \bar{q}_i q_j$  transition at the quark level, where  $\bar{q}_i = \bar{u}, \bar{c}$  and  $q_j = d, s$ , with  $\bar{c}$  antiquark remaining a spectator. In the

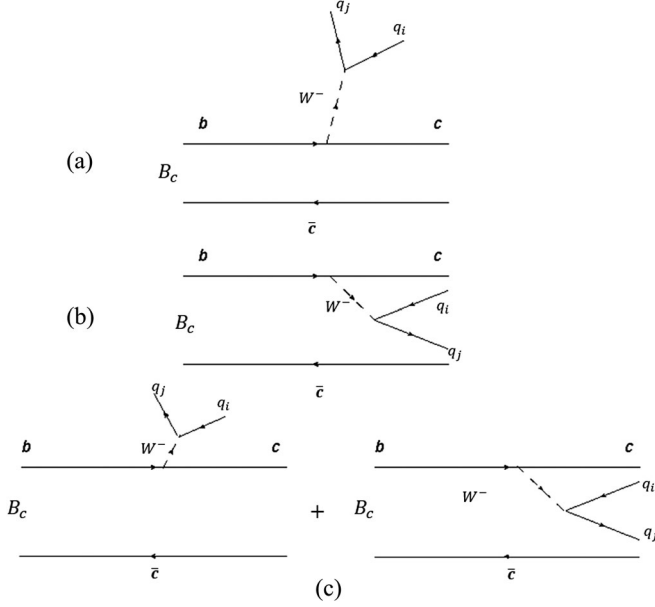


FIG. 1. Quark-level diagram of nonleptonic decay of meson  $B_c \rightarrow X_{c\bar{c}}(nS)M$ . (a) color-favored class I, (b) color-suppressed class II, and (c) class III decays.

present study, we restrict our discussion to class I and class III  $B_c$ -decay modes: each mode involving either  $\eta_c(nS)$  or  $\psi(nS)$  in the final state.

In fact, the decay process physically occurs in the momentum eigenstates of participating mesons. Therefore, in a field-theoretic description of the decay process, it is appropriate to represent the meson bound state in terms of a momentum wave packet reflecting momentum and spin distribution between a constituent quark and antiquark in the meson core. In the RIQ model, the wave packet corresponding to a meson bound state  $|B_c(\vec{p}, S_{B_c})\rangle$ , for example, at a definite moment  $\vec{p}$  and spin state  $S_{B_c}$ , is represented by

$$\begin{aligned} |B_c(\vec{p}, S_{B_c})\rangle &= \hat{\Lambda}(\vec{p}, S_{B_c})|(\vec{p}_b, \lambda_b); (\vec{p}_c, \lambda_c)\rangle \\ &= \hat{b}_b^\dagger(\vec{p}_b, \lambda_b)\hat{b}_c^\dagger(\vec{p}_c, \lambda_c)|0\rangle, \end{aligned} \quad (16)$$

where  $|(\vec{p}_b, \lambda_b); (\vec{p}_c, \lambda_c)\rangle$  is the Fock-space representation of the unbound quark and antiquark in a color-singlet configuration with respective momentum and spin:  $(\vec{p}_b, \lambda_b)$  and  $(\vec{p}_c, \lambda_c)$ .  $\hat{b}_q^\dagger(p_b, \lambda_b)$  and  $\hat{b}_c^\dagger(\vec{p}_c, \lambda_c)$  are the quark and antiquark creation operators. Here,  $\hat{\Lambda}(\vec{p}, S_{B_c})$  is a baglike integral operator taken in the form

$$\begin{aligned} \hat{\Lambda}(\vec{p}, S_{B_c}) &= \frac{\sqrt{3}}{\sqrt{N(\vec{p})}} \sum_{\lambda_b, \lambda_c} \zeta_{b,c}^{B_c}(\lambda_b, \lambda_c) \int d^3 p_b d^3 p_c \delta^{(3)} \\ &\times (\vec{p}_b + \vec{p}_c - \vec{p}) \mathcal{G}_{B_c}(\vec{p}_b, \vec{p}_c). \end{aligned} \quad (17)$$

Here,  $\sqrt{3}$  is the effective color factor, and  $\zeta_{b,c}^{B_c}(\lambda_b, \lambda_c)$  is the SU(6) spin-flavor coefficients for the  $B_c$ -meson state.

Imposing the normalization condition in the form  $\langle B_c(\vec{p}) | B_c(\vec{p}') \rangle = \delta^{(3)}(\vec{p} - \vec{p}')$ , the meson state normalization  $N(\vec{p})$  is obtainable in an integral form

$$N(\vec{p}) = \int d^3 \vec{p}_b |\mathcal{G}_{B_c}(\vec{p}_b, \vec{p} - \vec{p}_b)|^2. \quad (18)$$

Finally,  $\mathcal{G}_{B_c}(\vec{p}_b, \vec{p} - \vec{p}_b)$  denotes the momentum distribution function for the quark and antiquark pair in the meson core. In this model,  $\mathcal{G}_{B_c}(\vec{p}_b, \vec{p} - \vec{p}_b)$  is taken in the form  $\mathcal{G}_{B_c}(\vec{p}_b, \vec{p} - \vec{p}_b) = \sqrt{G_b(\vec{p}_b)G_c(\vec{p} - \vec{p}_b)}$  in the straightforward extension of the ansatz of Margolis and Mendel in their bag model description [60], where  $G_b(\vec{p}_b)$  and  $G_c(\vec{p} - \vec{p}_b)$  refer to the individual momentum probability amplitude of the constituent quark. Here, the effective momentum distribution function in fact embodies the bound-state character of  $|B_c(\vec{p}, S_{B_c})\rangle$ .

Any residual internal dynamics responsible for the decay process can, therefore, be described at the constituent level by the otherwise unbound quark and antiquark using usual Feynman technique. The constituent-level  $S$ -matrix element  $S_{fi}^{b \rightarrow c \bar{q}_i q_j}$  obtained from the appropriate Feynman diagram when operated upon by the bag like operator  $\hat{\Lambda}(\vec{p}, S_{B_c})$  (17) can give rise to the mesonic-level  $S$  matrix in the form

$$S_{fi}^{B_c \rightarrow X_{c\bar{c}}(nS)M} \rightarrow \hat{\Lambda}(\vec{p}, S_{B_c}) S_{fi}^{b \rightarrow c \bar{q}_i q_j}. \quad (19)$$

### A. $B_c \rightarrow P_1 P_2$

The nonleptonic decay mode,  $B_c \rightarrow P_1 P_2$ , where  $P_1$  and  $P_2$  are pseudoscalar mesons, [Fig. 1(a)], is induced by the  $b \rightarrow c \bar{q}_i q_j$  transition at quark level with the emission of a  $W$  boson. The resulting quark  $c$  and the spectator antiquark  $\bar{c}$  attached to the decaying meson state  $|B_c(\vec{p}, S_{B_c})\rangle$  hadronize to form  $|P_1(\vec{k}, S_{P_1})\rangle$ , while the externally emitted  $W$  boson with four momentum  $q$ , which decays to a quark-antiquark pair, subsequently hadronize to form the pseudoscalar meson state  $|P_2(\vec{q}, S_{P_2})\rangle$ . Considering the wave packet representation of the participating meson states in the factorized decay amplitude (3), the  $S$ -matrix element for  $B_c \rightarrow P_1 P_2$  can be obtained in the general form,

$$S_{fi} = (2\pi)^4 \delta^{(4)}(p - q - k) (-i\mathcal{M}_{fi}) \times \frac{1}{\sqrt{V2E_{B_c}}} \prod_f \frac{1}{\sqrt{V2E_f}}. \quad (20)$$

The invariant transition amplitude  $\mathcal{M}_{fi}$  is in fact extracted in the form

$$\mathcal{M}_{fi} = \frac{G_F}{\sqrt{2}} V_{bc} V_{\bar{q}_i q_j} a_1 A, \quad (21)$$

where  $A = h^\mu H_\mu$  with

$$h^\mu = \sqrt{\frac{2E_{P_2}}{(2\pi)^3}} \langle P_2(\vec{q}, S_{P_2}) | J^\mu | 0 \rangle \quad (22)$$

and

$$H_\mu = \frac{1}{\sqrt{N_{B_c}(\vec{p}) N_{P_1}(\vec{k})}} \int \frac{d^3 \vec{p}_b G_{B_c}(\vec{p}_b, \vec{p} - \vec{p}_b) G_{P_1}(\vec{p}_b + \vec{k} - \vec{p}, \vec{p} - \vec{p}_b)}{\sqrt{E_b(\vec{p}_b) E_c(\vec{p}_b + \vec{k} - \vec{p})}} \\ \times \sqrt{[E_b(\vec{p}_b) + E_c(\vec{p} - \vec{p}_b)][E_c(\vec{p}_b + \vec{k} - \vec{p}) + E_{\bar{c}}(\vec{p} - \vec{p}_b)]} \langle S_{P_1} | J_\mu(0) | S_{B_c} \rangle. \quad (23)$$

Here,  $E_b(\vec{p}_b)$  and  $E_c(\vec{p}_b + \vec{k} - \vec{p})$  stand for energy of the nonspectator quark of the parent and daughter meson;  $\vec{p}_b, \vec{p}, \vec{k}$  represent the three momentum of the nonspectator constituent quark  $b$ , parent meson  $B_c$ , and the daughter meson  $P_1$ , respectively.  $q = p - k$  is equal to the four momentum associated with the meson state  $|P_2(\vec{q}, S_{P_2})\rangle$ .  $\langle S_{P_1} | J_\mu | S_{B_c} \rangle$  represents symbolically the spin matrix elements of the effective vector-axial vector current. For transitions involving nonspectator constituent quark  $b$ , the spin matrix element is

$$\langle S_{P_1} | J_\mu | S_{B_c} \rangle = \sum_{\lambda_b, \lambda_c, \lambda_{\bar{c}}} \zeta_{b, \bar{c}}^{B_c}(\lambda_b, \lambda_{\bar{c}}) \zeta_{c, \bar{c}}^{P_1}(\lambda_c, \lambda_{\bar{c}}) \bar{u}_c \\ \times (\vec{p}_b + \vec{k} - \vec{p}, \lambda_c) \gamma_\mu (1 - \gamma_5) u_b(\vec{p}_b, \lambda_b). \quad (24)$$

Here,  $u_i$  stands for free Dirac spinor.  $\zeta_{b, \bar{c}}^{B_c}(\lambda_b, \lambda_{\bar{c}})$  and  $\zeta_{c, \bar{c}}^{P_1}(\lambda_c, \lambda_{\bar{c}})$  are the appropriate SU(6) spin-flavor coefficients corresponding to the parent and daughter mesons, respectively.

It may be pointed out here that in the description of any decay process, for example,  $B_c \rightarrow P_1 P_2$  in the RIQ model framework, the three momentum conservation is ensured explicitly via  $\delta^{(3)}(\vec{p}_q + \vec{p}_{\bar{q}_2} - \vec{p})$  in the participating meson states. However, energy conservation in such a scheme is not ensured so explicitly. This is in fact a typical problem in all potential model descriptions of mesons as a bound states of valence quarks and antiquarks interacting via some instantaneous potential. This problem has been addressed in our previous analysis in the context of radiative leptonic decays of heavy flavored means  $B, B_c, D, D_s$  [38], where the effective momentum distribution function  $\mathcal{G}_M(\vec{p}_{q_1}, \vec{p}_{\bar{q}_2})$  that embodies the bound-state characteristics of the meson ensures energy conservation in an average sense satisfying  $E_M = \langle M(\vec{p}, S_M) | [E_{q_1}(\vec{p}_{q_1}) + E_{\bar{q}_2}(\vec{p}_{\bar{q}_2})] | M(\vec{p}, S_M) \rangle$ . In view of this, we take the energy conservation constraint  $M = E_{q_1}(\vec{p}_{q_1}) + E_{\bar{q}_2}(-\vec{p}_{\bar{q}_1})$ , where  $M$  denotes the mass of the decaying meson at rest. This along with the three

momentum conservation via appropriate  $\delta^{(3)}(\vec{p}_{\bar{q}_1} + \vec{p}_{q_2} - \vec{p})$  in the meson state ensures the required four momentum conservation  $\delta^{(4)}(p - k - q)$  at the mesonic level, which is pulled out of the quark-level integration so as to obtain the  $S$ -matrix element in the standard form (20). This has been discussed elaborately in our earlier work [47].

Since the axial vector current does not contribute to the decay amplitude in the decay processes,  $B_c \rightarrow P_1 P_2$ , the only nonvanishing vector current part of (23) is simplified after calculating corresponding spin matrix elements (24) using usual spin algebra. The resulting timelike and space-like part of the hadronic matrix element in the parent meson rest frame are obtained, respectively, as

$$\langle P_1(\vec{k}) | V_0 | B_c(0) \rangle = H_0 = \int d\vec{p}_b C(\vec{p}_b) \{ [E_b(\vec{p}_b) + m_b] \\ \times [E_{\bar{c}}(\vec{p}_b + \vec{k}) + m_{\bar{c}}] + \vec{p}_b^2 \} \quad (25)$$

and

$$\langle P_1(\vec{k}) | V_i | B_c(0) \rangle = H_i = \int d\vec{p}_b C(\vec{p}_b) [E_b(\vec{p}_b) + m_b] k_i, \quad (26)$$

where

$$C(\vec{p}_b) = \frac{\mathcal{G}_{B_c}(\vec{p}_b, -\vec{p}_b) \mathcal{G}_{P_1}(\vec{p}_b + \vec{k}, -\vec{p}_b)}{\sqrt{N_{B_c}(0) N_{P_1}(\vec{k})}} \\ \times \sqrt{\frac{[E_b(\vec{p}_b) + E_{\bar{c}}(-\vec{p}_b)][E_c(\vec{p}_b + \vec{k}) + E_{\bar{c}}(-\vec{p}_b)]}{E_b(\vec{p}_b) E_c(\vec{p}_b + \vec{k}) [E_b(\vec{p}_b) + m_b] [E_c(\vec{p}_b + \vec{k}) + m_{\bar{c}}]}}. \quad (27)$$

Now, a comparison of the results [(25)–(27)] with the corresponding expression of the covariant factorized amplitude [(6)–(8)] yields the Lorentz invariant form factors  $f_\pm(q^2)$  in the form

$$f_{\pm}(q^2) = \frac{1}{2} \int d\vec{p}_b C(\vec{p}_b) \{ [E_b(\vec{p}_b) + m_b] \\ \times [E_c(\vec{p}_b + \vec{k}) + m_c] + \vec{p}_b^2 \\ \pm [E_b(\vec{p}_b) + m_b][M \mp E_{P_1}] \}. \quad (28)$$

Then, it is straightforward to get the model expression for the form factor  $F_0(q^2)$  from  $F_0(q^2) = \left[ \frac{q^2}{(M^2 - m_{P_1}^2)} \right] \times f_-(q^2) + f_+(q^2)$  in terms of which the decay rate  $\Gamma(B_c \rightarrow P_1 P_2)$  is obtained as

$$\Gamma(B_c \rightarrow P_1 P_2) = \frac{|\vec{k}|}{8\pi M^2} |A_1|^2 |F_0(q^2)|^2, \quad (29)$$

where

$$|A_1| = \frac{G_F}{\sqrt{2}} V_{bc} V_{\bar{q}_i q_j} a_1 (M^2 - m_{P_1}^2) f_{P_2}. \quad (30)$$

### B. $B_c \rightarrow PV$

In the nonleptonic decay process  $B_c \rightarrow PV$  of the class I category, the externally emitted  $W$  boson first decays to a quark-antiquark pair which ultimately hadronizes to a vector meson ( $V$ ), and the  $c$  quark originating from the nonspectator  $b$  decay along with the spectator  $\bar{c}$  hadronize to the pseudoscalar meson ( $P$ ) forming a member of the charmonium family. It can be readily checked that the decay amplitude in the  $B_c$  rest frame in such decays is obtainable in terms of the invariant form factor  $F_1(q^2)$  as

$$\langle P(\vec{k}) V(\vec{q}) | \mathcal{H}_{\text{eff}} | B_c(0) \rangle \\ = i \frac{G_F}{\sqrt{2}} V_{bc} V_{\bar{q}_i q_j} 2a_1 m_V f_V F_1(q^2) (e^* \cdot p). \quad (31)$$

Here,  $e^*$  denotes the polarization vector associated with the daughter meson ( $V$ ). The form factor  $F_1(q^2)$  in the parent meson rest frame is obtained as

$$F_1(q^2) = f_+(q^2) = \frac{1}{2} \int d\vec{p}_b C(\vec{p}_b) \{ [E_b(\vec{p}_b) \\ + m_b] [E_c(\vec{p}_b + \vec{k}) + m_c] + \vec{p}_b^2 \\ + [E_b(\vec{p}_b) + m_b][M - E_P] \}, \quad (32)$$

in terms of which the decay rate  $\Gamma(B_c \rightarrow PV)$  is expressed as

$$\Gamma(B_c \rightarrow PV) = \frac{|\vec{k}|^3}{8\pi m_V^2} |A_2|^2 |F_1(q^2)|^2, \quad (33)$$

where

$$|A_2| = \frac{G_F}{\sqrt{2}} V_{bc} V_{\bar{q}_i q_j} 2a_1 m_V f_V. \quad (34)$$

### C. $B_c \rightarrow VP$

In the decay process of this category, the externally emitted  $W$  boson first decays to a quark-antiquark pair which ultimately hadronizes to a pseudoscalar meson ( $P$ ). The resulting  $c$  from the nonspectator  $b$  decay and the spectator  $\bar{c}$  hadronize to the vector meson ( $V$ ) belonging to the charmonium family. In this case, the vector current does not contribute, and the nonvanishing decay amplitude due to axial-vector current in  $B_c$  rest frame is obtained in a simple form

$$\langle V(\vec{k}) P(\vec{q}) | \mathcal{H}_{\text{eff}} | B_c(0) \rangle \\ = i \frac{G_F}{\sqrt{2}} V_{bc} V_{\bar{q}_i q_j} 2a_1 m_V f_P A_0(q^2) (e^* \cdot p). \quad (35)$$

Although all four invariant form factors  $A_1, A_2, A_3,$  and  $A_0$  are expected to contribute to the decay amplitude in these decays, the contribution of a single form factor  $A_0(q^2)$  is relevant here as shown in (35). This is due to the mutual cancellation of terms arising from the linear relation (11). With the appropriate wave packet representation of the participating meson states  $|V(\vec{k}, S_V)\rangle$  and  $|B_c(0, S_{B_c})\rangle$ , the nonvanishing factorized amplitude  $\langle V(\vec{k}, S_V) | A_\mu | B_c(0, S_{B_c}) \rangle$  is calculated with respect to three spin states ( $S_V = \pm 1, 0$ ) of the vector meson ( $V$ ) in the final state. In the calculation of the spin matrix element, the polarization vector  $e^*$  associated with the final state vector meson is extracted from the model dynamics. The model expressions of the timelike and spacelike parts of the decay amplitude are then obtained in the parent meson rest frame as

$$\langle V(\vec{k}, S_V) | A_0 | B_c(0, S_{B_c}) \rangle \\ = \int d\vec{p}_b C(\vec{p}_b) [E_b(\vec{p}_b) + m_b] (\hat{e}^* \cdot \vec{k}) \quad (36)$$

and

$$\langle V(\vec{k}, S_V) | A_i | B_c(0, S_{B_c}) \rangle = \int d\vec{p}_b C(\vec{p}_b) \left\{ [E_b(\vec{p}_b) + m_b] \right. \\ \left. \times [E_c(\vec{p}_b + \vec{k}) + m_c] - \frac{\vec{p}_b^2}{3} \right\} \hat{e}^*, \quad (37)$$

respectively. A comparison of the expressions in (36) and (37) with the covariant expansions (9) and (10) leads to the model expression of the relevant form factor  $A_0(q^2)$  as

$$A_0(q^2) = \frac{1}{2} \int d\vec{p}_b C(\vec{p}_b) \left\{ [E_b(\vec{p}_b) + m_b][M - E_V] \right. \\ \left. \times [E_b(\vec{p}_b) + m_b][E_c(\vec{p}_b + \vec{k}) + m_c] - \frac{\vec{p}_b^2}{3} \right\}. \quad (38)$$

Then, the decay rate  $\Gamma(B_c \rightarrow VP)$  in terms of  $A_0(q^2)$  is obtained in a straightforward manner as

$$\Gamma(B_c \rightarrow VP) = \frac{|\vec{k}|^3}{8\pi m_V^2} |A_3|^2 |A_0(q^2)|^2, \quad (39)$$

where

$$|A_3| = \frac{G_F}{\sqrt{2}} V_{bc} V_{\bar{q}q} 2a_1 m_V f_P. \quad (40)$$

The two-body nonleptonic  $B_c$  decay described so far in this section refers to the color-favored “class I” decays involving external emission of a  $W$  boson [Fig. 1(a)]. For class III decay modes considered in the present study, the contribution to the decay amplitude is extracted from the Pauli interference of both the diagrams depicting external and internal emissions of a  $W$  boson. The model expressions for relevant form factors and decay rates for such decays can be obtained by suitably replacing the relevant flavor degree of freedom, quark masses, quark binding energies, QCD factors  $a_1$ ,  $a_2$ , and the decay constants.

#### IV. NUMERICAL RESULTS AND DISCUSSION

For calculating the two-body nonleptonic  $B_c$  decays in the relativistic independent quark (RIQ) model, we need to fix the flavor-independent potential parameters ( $a$ ,  $V_0$ ), quark masses ( $m_q$ ), and corresponding quark binding energy ( $E_q$ ). In fact, these parameters have already been fixed in our model in reproducing the experimental meson spectra in the light and heavy flavor sectors [39] and subsequently used in the description of wide ranging hadronic phenomena [40–47] involving participating mesons in their ground state. Accordingly, the potential parameters used in the present study are

$$(a, V_0) = (0.17166 \text{ GeV}^3, -0.1375 \text{ GeV}). \quad (41)$$

The quark masses and corresponding binding energies in GeV are taken as

$$\begin{aligned} m_u = m_d = 0.07875, \quad E_u = E_d = 0.47125, \\ m_s = 0.31575, \quad E_s = 0.591, \\ m_c = 1.49275, \quad E_c = 1.57951, \\ m_b = 4.77659, \quad E_b = 4.76633. \end{aligned} \quad (42)$$

For relevant CKM parameters and the lifetime of a  $B_c$  meson, we take their central values from PDG [61] as

$$\begin{aligned} |V_{cb}| = 0.041, \quad |V_{ud}| = 0.9737, \quad |V_{cs}| = 0.987, \\ |V_{us}| = 0.2245, \quad |V_{cd}| = 0.221, \quad \tau(B_c) = 0.51 \text{ ps}. \end{aligned} \quad (43)$$

For the masses and decay constants of the participating mesons, considered as phenomenological inputs in the present calculation, we take their central values of the available observed data from Refs. [61–63]. In the absence of the observed data in the charmonium and charm meson sectors, we take the corresponding predicted values from established theoretical approaches [64–67]. Accordingly, the updated meson masses and decay constants used in the present analysis are listed in Table I.

Note that, in the prediction of nonleptonic decays, uncertainties creep into the calculation through input parameters: model parameters, CKM parameters, meson decay constants, and QCD coefficients ( $a_1$ ,  $a_2$ ), etc. As mentioned above, we use in our calculation the potential parameters (41) and the quark masses and quark binding energies (42) that have already been fixed at the static-level application of the RIQ model by fitting the mass spectra of mesons in their ground state [39]. The same set of parameters has been used in earlier application of RIQ

TABLE I. The masses and decay constants of mesons.

Particle	Mass [61] (MeV)	Decay constant (MeV)	References
$\pi$	139.57	130.5	[61]
$\rho$	775.11	221	[61]
$K^\pm$	493.677	155.72	[61]
$K^{*\pm}$	891.67	220	[61]
$D^\pm(1S)$	1869.5	205.8	[61]
$D^*(1S)$	2010.2	252.2	[66]
$D_s^\pm(1S)$	1968.35	252.4	[61]
$D_s^{*\pm}(1S)$	2112.2	305.5	[66]
$\eta_c(1S)$	2983.9	387	[67]
$J/\psi(1S)$	3096.9	418	[67]
$B_c$	6274.47		
Particle	Mass (MeV)	References	
$D(2S)$	2581	[64]	
$D^{*\pm}(2S)$	2637	[62]	
$D_s(2S)$	2673	[64]	
$D_s^*(2S)$	2732	[63]	
$\eta_c(2S)$	3637.	[61]	
$\psi(2S)$	3686.1	[61]	
$D^\pm(3S)$	3068	[64]	
$D^{\pm*}(3S)$	3110	[64]	
$D_s^\pm(3S)$	3154	[64]	
$D_s^{*\pm}(3S)$	3193	[64]	
$\eta_c(3S)$	4007	[65]	
$\psi(3S)$	4039.1	[61]	

model yielding adequate descriptions of wide ranging hadronic phenomena in the light and heavy flavor mesons in their ground state. Subsequently, we extend our model application to study the  $B_c$ -meson decays into radially excited daughter mesons [43]. In the calculation of such decay processes [43], we use the same set of input parameters [(41), (42)] except the quark binding energies. The quark binding energies for excited meson states are obtained by solving the equation representing appropriate binding energy condition in our model. As such, we do not use any free parameters that could be fine-tuned from time to time to predict wide ranging hadronic phenomena as stated above. In that sense, we perform parameter-free calculations in our studies. In order to avoid uncertainties that might creep into our calculation through the CKM parameters and decay constants, we take their central values of the observed data from Ref. [61]. In those cases where observed data for decay constants are not available, we use the predicted data from established model and theoretical approaches [66,67]. Regarding the QCD coefficient ( $a_1, a_2$ ), different numerical values have been used in the literature in the calculation of the nonleptonic transitions of  $B_c$  mesons induced by  $b$ -quark decay. For example Colangelo and De Fazio, in Ref. [27] use QCD coefficients, Set 1:  $(a_1^b, a_2^b) = (1.12, -0.26)$ , as fixed in Ref. [68]. In most earlier calculations, the authors use a different set of QCD coefficients, Set 2:  $(a_1^b, a_2^b) = (1.14, -0.2)$ , fixed by Buras *et al.* [52] in the mid 1980s, whereas Dubnicka *et al.* [37] use a different set of numerical values, i.e., Set 3:  $(a_1^b, a_2^b) = (0.93, -0.27)$ . We use all three sets of the Wilson coefficients in our calculation.

Before calculating invariant form factors using our input parameters [(41), (42)], we would like to elaborate a bit on the energy conservation ansatz discussed in Sec. III to ensure the required energy-momentum conservation in our description of nonleptonic  $B_c$ -meson decays. Considering a meson state  $|X(0)\rangle$  decaying at rest, the energy conservation constraint  $M = E_{q_1}(\vec{p}_{q_1}) + E_{q_2}(-\vec{p}_{q_1})$  might lead to spurious kinematic singularities at the quark-level integration that appear in the decay amplitude. This problem has been addressed in our model analysis on radiative leptonic decays of heavy flavored mesons [41] and in similar studies based on the QCD relativistic quark model approach [27] by assigning a running mass to the nonspectator quark  $q_1$ ,

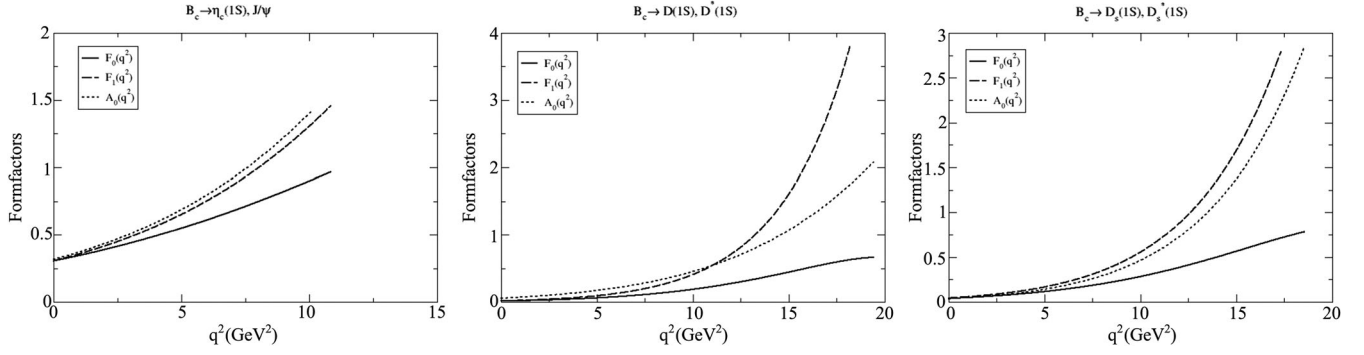
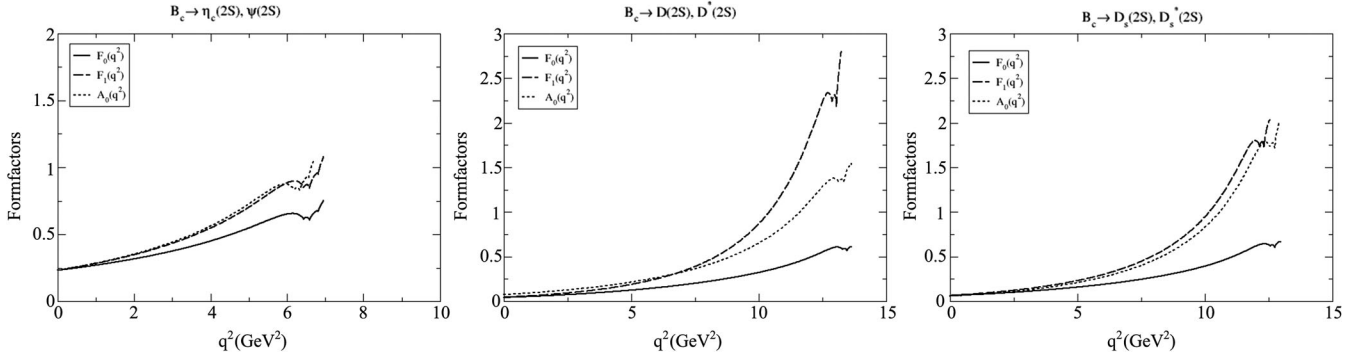
$$m_{q_1}^2(|\vec{p}_{q_1}|) = M^2 - m_{q_2}^2 - 2M\sqrt{|\vec{p}_{q_1}|^2 + m_{q_2}^2},$$

as an outcome of the energy conservation ansatz, while retaining definite mass  $m_{q_2}$  of the spectator quark  $\bar{q}_2$ . This leads to an upper bound on the quark momentum  $|\vec{p}_{q_1}| < \frac{M^2 - m_{q_2}^2}{2M}$  in order to retain  $m_{q_1}^2(|\vec{p}_{q_1}|)$  positive definite. The shape of the radial momentum distribution amplitude  $|\vec{p}_{q_1}| \mathcal{G}_X(\vec{p}_{q_1}, -\vec{p}_{q_1})$  over the allowed kinematic range  $0 \leq |\vec{p}_{q_1}| < |\vec{p}_{q_1}|_{\max}$  as shown in Figs. 5–7 also match with the shape obtained in similar studies in the QCD relativistic quark model approach [27]. The rms value of the active quark momentum  $\sqrt{\langle |\vec{p}_{q_1}^2| \rangle}$ , where  $\langle |\vec{p}_{q_1}^2| \rangle = \langle X(0) | \vec{p}_{q_1}^2 | X(0) \rangle$ , the expectation value of the binding energies of the active quark  $q_1$ , and spectator  $q_2$  and sum of the binding energy of quark and antiquark pair  $\langle E_{q_1}(\vec{p}_{q_1}^2) \rangle$ ,  $\langle E_{q_2}(|-\vec{p}_{q_1}|^2) \rangle$ , and  $\langle E_{q_1}(\vec{p}_{q_1}^2) + E_{q_2}(|-\vec{p}_{q_1}|^2) \rangle$ , respectively, calculated in the framework of RIQ model, are presented in Table II.

It is note worthy to discuss three important aspects of our results in Table II. (1) The rms value of the quark momentum in the meson bound state is much less than the corresponding upper bound  $|\vec{p}_{q_1}|_{\max}$  as expected. (2) The average energy of a constituent quark of the same flavor in different meson bound states does not exactly match. This is because the kinematics and binding energy condition for constituent quarks due to the color forces involved are different from one meson bound state to other. The constituent quarks in the meson bound state are considered to be free particles of definite momenta, each associated with its momentum probability amplitude derivable in this model via momentum space projection of the respective quark eigenmodes. On the other hand the energies shown in Eq. (42), which are the energy eigenvalues of the corresponding bound quarks with no definite momenta of their own, are obtained in the RIQ model from respective quark orbitals by solving the Dirac equation. It is no wonder that we find the marginal difference between the energy eigenvalues (42) and average energy of constituent quarks shown in Table II. (3) Finally, we obtained the expectation values of the sum of the energy of a constituent quark and antiquark in the meson bound state in good agreement with corresponding observed masses as shown

TABLE II. The rms values of quark momentum, expectation values of the quark and antiquark, and expectation value of sum of the quark and antiquark pair in the meson states.

Meson state $ X(0)\rangle$	$\sqrt{\langle \vec{p}_{q_1}^2 \rangle}$ (GeV)	$\langle E_{q_1}(\vec{p}_{q_1}^2) \rangle$ (GeV)	$\langle E_{q_2}( -\vec{p}_{q_1} ^2) \rangle$ (GeV)	$\langle [E_{q_1}(\vec{p}_{q_1}^2) + E_{q_2}( -\vec{p}_{q_1} ^2)] \rangle$ (GeV)	Observed meson mass (GeV)
$ B_u(0)\rangle$	0.51	4.799	0.480	5.279	5.27925
$ B_c(0)\rangle$	0.66	4.657	1.629	6.286	6.27447
$ D(0)\rangle$	0.4506	1.4418	0.4275	1.8693	1.86965
$ D_s(0)\rangle$	0.4736	1.4165	0.5517	1.9682	1.96835


 FIG. 2.  $q^2$  dependence of the form factors in the nonleptonic  $B_c$  decays to a final meson in the 1S state.

 FIG. 3.  $q^2$  dependence of the form factors in the nonleptonic  $B_c$  decays to a final meson in the 2S state.

in Table II. These important aspects of our results lend credence to our energy conservation ansatz in an average sense through an effective momentum distribution function like  $\mathcal{G}_X(\vec{p}_{q_1}, -\vec{p}_{q_1})$  in the meson bound state  $|X(0)\rangle$ . This ansatz along with three momentum conservation in the meson bound state ensures the required energy momentum conservation in our description of several decay processes [39–47] as pointed out earlier. In the absence of any rigorous field theoretic description of the meson bound states, invoking such an ansatz is no doubt a reasonable approximation for a constituent-level description of hadronic phenomena.

With the input parameters [(41), (42)], we first study the  $q^2$  dependence of the form factors in the allowed kinematic

range  $0 < q^2 \leq q_{\max}^2$  from analytic expressions [(28), (32), (38)]. In a self-consistent dynamic approach, we extract the form factor from the overlapping integrals of meson wave functions wherein the  $q^2$  dependence is automatically encoded in relevant expressions. This is in contrast to some model approaches cited in the literature where the form factors are determined only at one kinematic point, i.e., at  $q^2 \rightarrow 0$  or  $q^2 \rightarrow q_{\max}^2$ , and then extrapolated to the entire kinematic range using some phenomenological ansatz (mainly dipole or Gaussian form). Our predicted  $q^2$  dependencies of the form factors  $F_0(q^2)$ ,  $F_1(q^2)$ , and  $A_0(q^2)$  for nonleptonic  $B_c$  decays to ground and radially excited meson states are depicted in Figs. 2–4. We find that the form factors relevant to the transitions to 1S meson

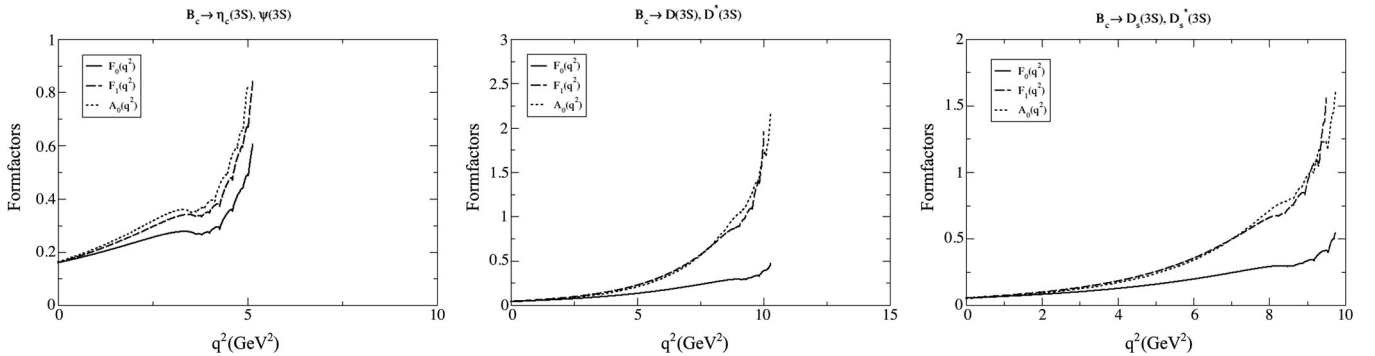

 FIG. 4.  $q^2$  dependence of the form factors in the nonleptonic  $B_c$  decays to a final meson in the 3S state.

TABLE III. The form factors ( $F_0, F_1, A_0$ ) at  $q^2 = 0$  evaluated in the RIQ model for exclusive nonleptonic  $B_c$  decays to  $1S, 2S, 3S$  final state mesons.

Form factors	Final meson state	$B_c \rightarrow \eta_c, J/\psi$	$B_c \rightarrow D, D^*$	$B_c \rightarrow D_s, D_s^*$
$F_0$	$1S$	0.3057	0.0163	0.040
$F_1$	$1S$	0.3058	0.018	0.045
$A_0$	$1S$	0.3164	0.058	0.038
$F_0$	$2S$	0.232	0.044	0.063
$F_1$	$2S$	0.232	0.046	0.066
$A_0$	$2S$	0.232	0.076	0.060
$F_0$	$3S$	0.160	0.043	0.054
$F_1$	$3S$	0.160	0.045	0.056
$A_0$	$3S$	0.163	0.0405	0.051

states increase with increasing  $q^2$  in the entire kinematic range. This behavior, however, is not universal as the  $q^2$  dependence pattern is found different for transitions to

radially excited  $2S$  and  $3S$  meson states. We also find that the form factors  $F_1(q^2)$  and  $A_0(q^2)$  dominate  $F_0(q^2)$  throughout the kinematic range for all transitions. In transitions to the higher excited ( $2S$  and  $3S$ ) states, the plots for  $F_1(q^2)$  and  $A_0(q^2)$  almost overlap throughout the kinematic range above  $F_0(q^2)$ . Our predicted form factors at maximum recoil point  $q^2 \rightarrow 0$  as listed in Table III also satisfy the requirement for pole cancellation in  $B_c \rightarrow P$  transitions.

Before evaluating the decay rates/branching fractions, it is interesting to plot the radial quark momentum distribution amplitude  $|\vec{p}_b| \mathcal{G}_{B_c}(\vec{p}_b, -\vec{p}_b)$  for a decaying  $B_c$  meson at rest in its ground state along with that for the daughter mesons in their ground as well as radially excited ( $2S$  and  $3S$ ) states over the allowed physical range of the quark momentum. From the plots shown in Figs. 5–7, we find that the overlap region in the transition to ground ( $1S$ ) state is maximum. However, the overlaps of momentum distribution amplitudes are found to decrease as one considers transitions to higher excited  $2S$  and  $3S$  states.

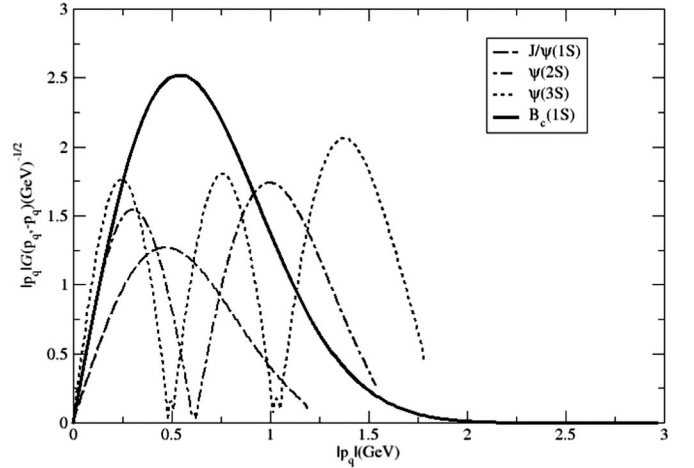
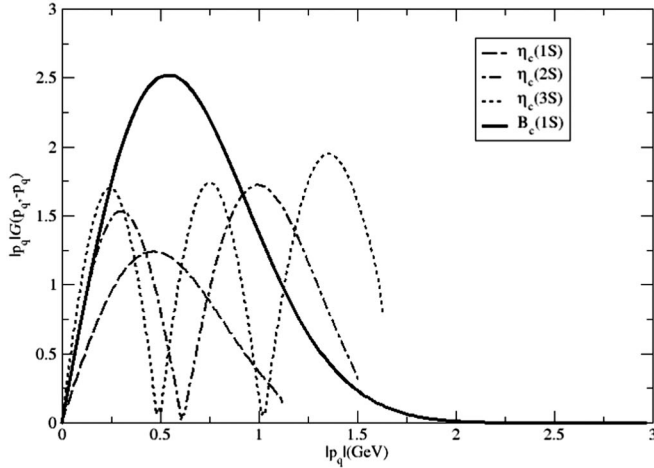


FIG. 5. Overlap of momentum distribution amplitudes of the initial and final meson states.

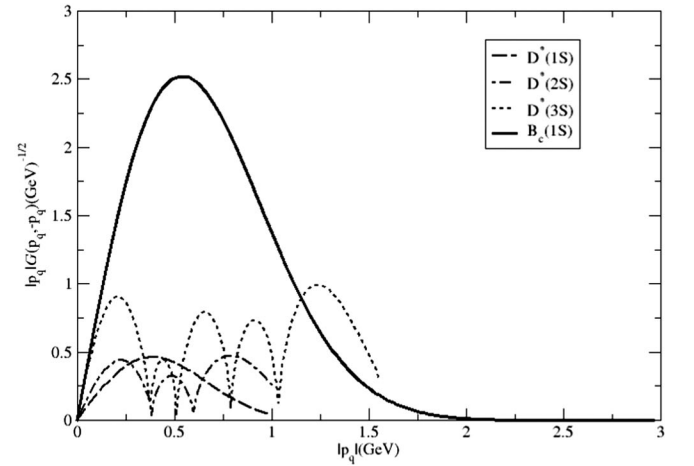
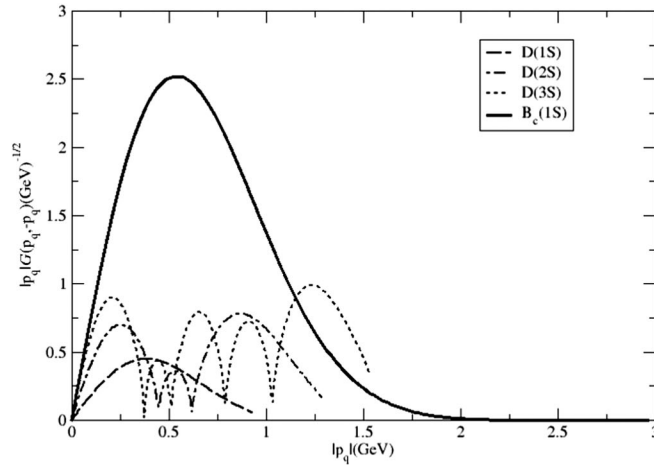


FIG. 6. Overlap of momentum distribution amplitudes of the initial and final meson states.

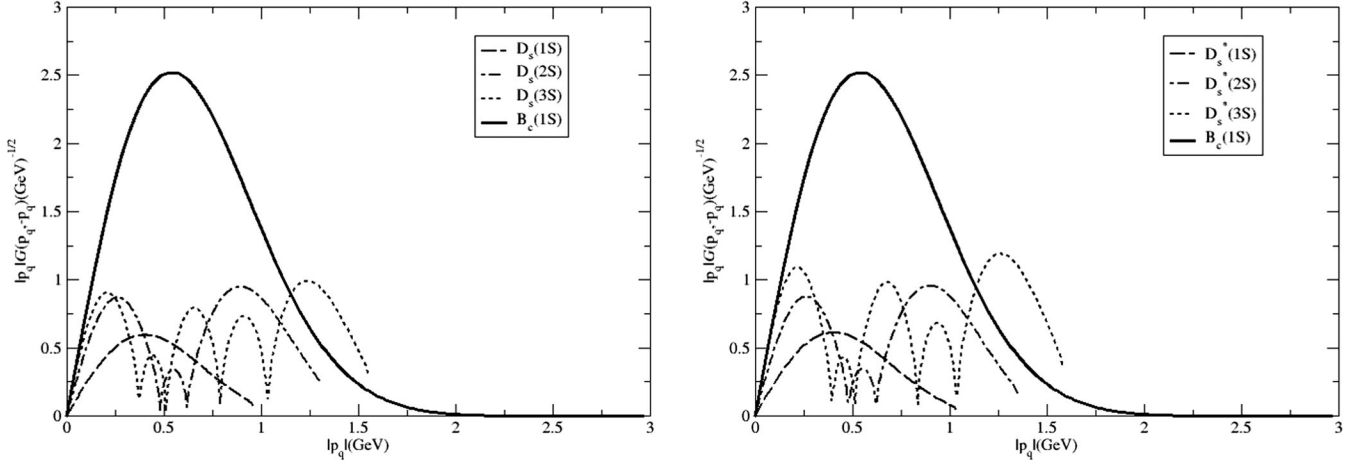


FIG. 7. Overlap of momentum distribution amplitudes of the initial and final meson states.

Since invariant form factors are extracted from overlapping integrals of participating meson wave functions, one expects the form factor contribution to the decay rate/branching fractions in the decreasing order of magnitude for transition to daughter mesons from their ground to higher excited states.

We then evaluate the decay rates from the expressions in Eqs. (29), (33), and (39), and our results for general values of QCD coefficients ( $a_1, a_2$ ) of the operator product expansion are listed in Table IV to facilitate a comparison with other dynamical model predictions.

Our predicted branching fractions for various tree-level two-body nonleptonic  $B_c$  decays to 1S, 2S, and 3S charmonium states in comparison with other model predictions are listed in Tables V, VI, and VII, respectively.

Our results for decays to 1S, 2S, and 3S final states corresponding to three sets of QCD parameters are listed in the second column of each table. As expected our predicted branching fractions are obtained in the following hierarchy:

$$\begin{aligned} \mathcal{B}(B_c \rightarrow X_{c\bar{c}}(3S)M) &< \mathcal{B}(B_c \rightarrow X_{c\bar{c}}(2S)M) \\ &< \mathcal{B}(B_c \rightarrow X_{c\bar{c}}(1S)M). \end{aligned}$$

Our results for transitions to 2S and 3S final states are found about two and three orders of magnitude smaller, respectively, than those for 1S final states. The node structure of the 2S wave function is responsible for small branching fractions. In the calculation of the overlap integral of meson wave functions, as there is no node for the initial wave functions, the positive and negative parts of the final wave function give contributions which cancel each other out yielding a small branching fraction. With regard to 3S final states, there are even more severe cancellations, which lead to still smaller branching fractions. As expected the tighter phase space and weaker  $q^2$  dependence of form factors also lead to smaller branching fractions for transitions to higher excited 2S and 3S final states.

 TABLE IV. Decay widths in units of  $10^{-15}$  GeV for general values of the Wilson coefficients ( $a_1, a_2$ ) in nonleptonic  $B_c$ -meson decays to 1S, 2S, and 3S charmonium states. For the sake of brevity, we use the notation  $\eta'_c, \psi' = \eta_c(2S), \psi(2S)$ ;  $\eta''_c, \psi'' = \eta_c(3S), \psi(3S)$ .

Decay	Width	Decay	Width	Decay	Width
$B_c^- \rightarrow \eta_c \pi$	$0.394a_1^2$	$B_c^- \rightarrow \eta'_c \pi$	$0.143a_1^2$	$B_c^- \rightarrow \eta''_c \pi$	$0.0485a_1^2$
$B_c^- \rightarrow \eta_c K$	$0.0312a_1^2$	$B_c^- \rightarrow \eta'_c K$	$0.0116a_1^2$	$B_c^- \rightarrow \eta''_c K$	$0.0039a_1^2$
$B_c^- \rightarrow \eta_c D$	$(0.306a_1 + 0.221a_2)^2$	$B_c^- \rightarrow \eta'_c D$	$(0.199a_1 + 0.3012a_2)^2$	$B_c^- \rightarrow \eta''_c D$	$(0.1009a_1 + 0.2325a_2)^2$
$B_c^- \rightarrow \eta_c D_s$	$(1.727a_1 + 1.478a_2)^2$	$B_c^- \rightarrow \eta'_c D_s$	$(1.135a_1 + 1.5558a_2)^2$	$B_c^- \rightarrow \eta''_c D_s$	$(0.512a_1 + 0.9910a_2)^2$
$B_c^- \rightarrow \eta_c \rho$	$1.237a_1^2$	$B_c^- \rightarrow \eta'_c \rho$	$0.450a_1^2$	$B_c^- \rightarrow \eta''_c \rho$	$0.1541a_1^2$
$B_c^- \rightarrow \eta_c K^*$	$0.0652a_1^2$	$B_c^- \rightarrow \eta'_c K^*$	$0.00237a_1^2$	$B_c^- \rightarrow \eta''_c K^*$	$0.0081a_1^2$
$B_c^- \rightarrow \eta_c D^*$	$(0.346a_1 + 0.2819a_2)^2$	$B_c^- \rightarrow \eta'_c D^*$	$(0.199a_1 + 0.3611a_2)^2$	$B_c^- \rightarrow \eta''_c D^*$	$(0.0662a_1 + 0.2059a_2)^2$
$B_c^- \rightarrow \eta_c D_s^*$	$(1.893a_1 + 1.720a_2)^2$	$B_c^- \rightarrow \eta'_c D_s^*$	$(1.062a_1 + 1.6054a_2)^2$	$B_c^- \rightarrow \eta''_c D_s^*$	$(0.313a_1 + 0.558a_2)^2$
$B_c^- \rightarrow J/\psi \pi$	$0.4949a_1^2$	$B_c^- \rightarrow \psi' \pi$	$0.173a_1^2$	$B_c^- \rightarrow \psi'' \pi$	$0.061a_1^2$
$B_c^- \rightarrow J/\psi K$	$0.0387a_1^2$	$B_c^- \rightarrow \psi' K$	$0.0136a_1^2$	$B_c^- \rightarrow \psi'' K$	$0.0045a_1^2$
$B_c^- \rightarrow J/\psi D$	$(0.306a_1 + 0.4784a_2)^2$	$B_c^- \rightarrow \psi' D$	$(0.178a_1 + 0.399a_2)^2$	$B_c^- \rightarrow \psi'' D$	$(0.0753a_1 + 0.2567a_2)^2$
$B_c^- \rightarrow J/\psi D_s$	$(1.697a_1 + 2.0503a_2)^2$	$B_c^- \rightarrow \psi' D_s$	$(0.9708a_1 + 1.964a_2)^2$	$B_c^- \rightarrow \psi'' D_s$	$(0.345a_1 + 0.3634a_2)^2$

TABLE V. Branching fractions (in %) of the  $B_c \rightarrow \eta_c X$  and  $B_c \rightarrow J/\psi P$  decays, where  $X = P, V$  in comparison with other model predictions.

Decay	This work			[22]	[24]	[27]	[31]	[32]	[33]	[34]	[35]	[36]	[38]
	$a_1 = 0.93$ $a_2 = -0.27$	$a_1 = 1.12$ $a_2 = -0.26$	$a_1 = 1.14$ $a_2 = -0.20$										
$B_c^- \rightarrow \eta_c \pi$	0.0264	0.0383	0.0397	...	0.083	0.025	0.094	0.13	0.14	0.20	0.18	0.189	0.19
$B_c^- \rightarrow \eta_c K$	0.002	0.003	0.0031	...	0.006	0.002	0.0075	0.013	0.011	0.013	0.014	0.015	0.015
$B_c^- \rightarrow \eta_c D^-$	0.0039	0.006	0.0068	...	...	0.005	0.014	0.010	0.014	0.015	0.0012	...	0.019
$B_c^- \rightarrow \eta_c D_s$	0.1128	0.1861	0.2169	...	...	0.50	0.44	0.35	0.26	0.28	0.054	...	0.44
$B_c^- \rightarrow \eta_c \rho$	0.0828	0.120	0.124	...	0.20	0.067	0.24	0.30	0.33	0.42	0.49	0.518	0.45
$B_c^- \rightarrow \eta_c K^*$	0.0043	0.0063	0.0065	...	0.011	0.004	0.013	0.021	0.018	0.02	0.025	0.029	0.025
$B_c^- \rightarrow \eta_c D^*$	0.0046	0.0076	0.0088	...	...	0.003	0.012	0.0055	0.013	0.010	0.0010	...	0.019
$B_c^- \rightarrow \eta_c D_s^*$	0.1301	0.216	0.254	...	...	0.057	0.24	0.36	0.24	0.27	0.044	...	0.37
$B_c^- \rightarrow J/\psi \pi$	0.0331	0.038	0.039	0.0664	0.06	0.13	0.076	0.073	0.11	0.13	0.18	0.101	0.17
$B_c^- \rightarrow J/\psi K$	0.0025	0.003	0.0031	0.00527	0.005	0.007	0.006	0.007	0.008	0.011	0.014	0.008	0.013
$B_c^- \rightarrow J/\psi D$	0.0018	0.00369	0.00496	0.00552	...	0.013	0.0083	0.0044	0.009	0.009	0.0009	...	0.015
$B_c^- \rightarrow J/\psi D_s$	0.0813	0.1449	0.1801	0.137	...	0.35	0.24	0.12	0.15	0.041	0.34	...	0.34

Our predictions for branching fractions corresponding to  $B_c$  decays to  $1S$  and  $2S$  final states are found in general agreement with some model predictions and differ from other model predictions by a factor of 2–3 as shown in Tables V and VI. There are a few theoretical predictions on the branching fractions for  $B_c$ -meson decays to higher  $3S$  states. Our predicted branching fractions with respect to three sets of Wilson coefficients are found comparable to the predictions based on the improved Bethe-Salpeter approach [29,30] as shown in Table VII.

Our prediction for  $B_c \rightarrow X_{c\bar{c}}(1S)M$  decays shown in Table V are in good agreement with the model predictions of Refs. [22,24,27,31], and those for class III transitions like  $B_c^- \rightarrow \eta_c D_s^-, B_c^- \rightarrow \eta_c D_s^*$ , and  $B_c^- \rightarrow J/\psi D_s^*$  moderately agree with those of Refs. [32–38]. For other decay modes, our results are about one order of magnitude smaller

than theirs. For  $B_c \rightarrow X_{c\bar{c}}(2S)M$  decays, our results as listed in Table VI also agree well with those of Refs. [22,23,25] and agree moderately with the results of Refs. [27,29,30]. Compared to the branching fractions for  $B_c \rightarrow \eta_c' \pi$  and  $B_c \rightarrow \psi' \pi$  predicted in the perturbative QCD approach based on  $k_T$  factorization [20], our results are found one order of magnitude smaller. Our predictions of  $B_c \rightarrow X_{c\bar{c}}(3S)M$  decays shown in Table VII are found comparable to those of the model calculation based on the improved Bethe-Salpeter approach [29,30], except for  $B_c \rightarrow \psi' D$  decay which is found one order of magnitude larger than theirs. The dominant decay modes to  $1S$  meson states are  $B_c \rightarrow \eta_c(\rho^-, D_s^-, D_s^{*-})$  and  $B_c \rightarrow J/\psi D_s^-$  which should be accessible at LHCb. The predicted branching fractions of decays to  $2S$  and  $3S$  states  $B_c \rightarrow \eta_c'(\rho^-, D_s^-, D_s^{*-})$ ,  $B_c \rightarrow \psi' D_s^-$ , and  $B_c \rightarrow \eta_c''(\rho^-, D_s^-, D_s^{*-})$ ,

TABLE VI. Branching fractions (in  $10^{-4}$ ) of the  $B_c^- \rightarrow \eta_c' X$  and  $B_c^- \rightarrow \psi' P$  decays, where  $X = P, V$  in comparison with other model predictions.

Decay	This work			[35]	[22]	[23]	[24]	[25]	[27]	[29,30]	[20]
	$a_1 = 0.93$ $a_2 = -0.27$	$a_1 = 1.12$ $a_2 = -0.26$	$a_1 = 1.14$ $a_2 = -0.20$								
$B_c^- \rightarrow \eta_c' \pi$	0.95	1.39	1.44	2.4	...	2.4	1.7	2.2	0.66	1.67	10.3
$B_c^- \rightarrow \eta_c' K$	0.077	0.11	0.117	0.18	...	0.18	0.125	0.16	$4.9 \times 10^{-2}$	0.119	...
$B_c^- \rightarrow \eta_c' D$	0.083	0.161	0.21	0.20	...	0.057	...	...	$2.2 \times 10^{-2}$	$3.19 \times 10^{-2}$	...
$B_c^- \rightarrow \eta_c' D_s$	3.12	5.81	7.4	8.7	...	0.67	...	...	0.785	4.47	...
$B_c^- \rightarrow \eta_c' \rho$	3.01	12.03	12.46	5.5	...	5.5	3.6	5.25	1.4	3.56	...
$B_c^- \rightarrow \eta_c' K^*$	0.15	0.23	0.239	0.28	...	0.26	0.15	0.25	$7.15 \times 10^{-2}$	0.191	...
$B_c^- \rightarrow \eta_c' D^*$	0.059	0.12	0.185	0.11	...	0.21	...	...	$7.8 \times 10^{-4}$	0.285	...
$B_c^- \rightarrow \eta_c' D_s^*$	2.37	4.61	6.13	4.4	...	4.5	...	...	0.20	3.56	...
$B_c^- \rightarrow \psi' \pi$	1.15	1.34	1.39	2.2	2.97	3.7	1.1	0.63	2.0	1.42	6.7
$B_c^- \rightarrow \psi' K$	0.091	0.105	0.109	0.16	0.23	0.29	$8 \times 10^{-2}$	$4.45 \times 10^{-2}$	$8.9 \times 10^{-2}$	0.102	...
$B_c^- \rightarrow \psi' D$	0.0258	0.07	0.11	0.11	0.138	0.24	...	...	$7.3 \times 10^{-2}$	$1.55 \times 10^{-2}$	...
$B_c^- \rightarrow \psi' D_s$	1.075	2.57	3.94	4.4	3.08	5.25	...	...	1.2	2.69	...

TABLE VII. Predicted branching fractions (in  $10^{-5}$ ) of the  $B_c \rightarrow \eta_c'' x$  and  $B_c \rightarrow \psi'' P$  where  $X = P, V$ .

Decay	This work			[29]	[30]
	$a_1 = 0.93$ $a_2 = -0.27$	$a_1 = 1.12$ $a_2 = -0.26$	$a_1 = 1.14$ $a_2 = -0.20$		
$B_c^- \rightarrow \eta_c'' \pi$	3.2	4.7	4.8	2.16	...
$B_c^- \rightarrow \eta_c'' K$	0.26	0.38	0.39	0.153	...
$B_c^- \rightarrow \eta_c'' D$	0.074	0.21	0.36	...	...
$B_c^- \rightarrow \eta_c'' D_s$	3.3	7.72	11.5	...	...
$B_c^- \rightarrow \eta_c'' \rho$	10.1	14.9	15.5	4.29	...
$B_c^- \rightarrow \eta_c'' K^*$	0.54	0.79	0.81	0.225	...
$B_c^- \rightarrow \eta_c'' D^*$	0.24	0.032	0.09	...	...
$B_c^- \rightarrow \eta_c'' D_s^*$	1.52	3.2	4.6	...	...
$B_c^- \rightarrow \psi'' \pi$	4.08	4.7	4.8	3.11	...
$B_c^- \rightarrow \psi'' K$	0.301	0.35	0.36	0.214	...
$B_c^- \rightarrow \psi'' D$	$0.04 \times 10^{-3}$	0.02	0.092	...	$3.67 \times 10^{-3}$
$B_c^- \rightarrow \psi'' D_s$	3.84	6.6	7.9	...	3.76

$B_c \rightarrow \psi'' D_s^-$  up to  $\sim 10^{-4}$  may be accessible at high luminosity hadron colliders in the near future. All other decays discussed in the present work cannot reach the detection ability of current experiments.

It is of interest to estimate the ratios of branching fractions of pairs of modes  $B_c \rightarrow PV$ ,  $B_c \rightarrow PP$ , and  $B_c \rightarrow VP$ ,  $B_c \rightarrow PP$  which are expected to be  $\approx 3$  from naive spin counting. We find that only for the pair  $B_c^- \rightarrow \eta_c(nS)\rho^-$  and  $B_c \rightarrow \eta_c(nS)\pi^-$  does the naive spin counting hold good. However, for all other pairs, we obtain approximate equality except for the pairs  $B_c^- \rightarrow \psi(nS)D_s^-$  and  $B_c^- \rightarrow \eta_c(nS)D_s^-$  where our predicted ratio shows an inversion of the spin counting ratio. The deviation of the naive spin counting is a common feature of all model predictions.

The relative size of branching fractions for nonleptonic  $B_c$  decays is broadly estimated from power counting of QCD factors in the Welfenstein parametrization [69]. Accordingly the class I decay modes determined by the QCD factor,  $a_1$  are found to have comparatively large branching fractions which should be measured experimentally. In class III decays, which are characterized by Pauli interference, the branching fractions are determined by the relative value of  $a_1$  with respect to  $a_2$ . Considering the positive value of  $a_1 = 1.12$  and negative value of  $a_2 = -0.26$  in Set 1, for example, used in the literature, this leads to destructive interference. As a result, the decay modes are found suppressed in comparison with the cases where interference is switched off. However, at the qualitative level, it is known that the ratio  $a_2/a_1$  is a function of running coupling constant  $\alpha_s$  evaluated at the factorization scale, which is shown to be positive in case of  $b$ -flavored meson decays corresponding to small coupling [54]. The experimental data also favor constructive interference of color-favored and color-suppressed  $B_c$ -decay modes. Considering positive value  $a_2^b = 0.26$ , our predicted

branching fractions for class III decays to 1S and 2S final states find enhancement by a factor  $\sim 2$  to 4 and  $\sim 3$  to 7, respectively, over that obtained with a negative value of  $a_2^b = -0.26$ . For decays to 3S final states, the enhancement is still more significant.

It is possible to study the effect of Pauli interference in class III  $B_c$  decays by casting the decay width in the form  $\Gamma = \Gamma_0 + \Delta\Gamma$ , where  $\Gamma_0 = x_1^2 a_1^2 + x_2^2 a_2^2$ ,  $\Delta\Gamma = 2x_1 x_2 a_1 a_2$ , and computing  $\frac{\Delta\Gamma}{\Gamma_0}$  in % as done in [47,48,55]. The absolute values of  $\frac{\Delta\Gamma}{\Gamma_0}$  for  $B_c$  decays to 1S final states are found in the range of 32.7% – 63.9%. Those for decay modes to 2S and 3S final states are obtained in the range of 57.7% – 82.6% and 46.2% – 97.3%, respectively. Thus, we find that interference is more significant in class III  $B_c$  decays to higher excited 2S and 3S states compared to those estimated for decays to 1S final states.

Finally, we predict the studied observable  $\mathcal{R}$ : ratios of branching fractions of the nonleptonic  $B_c$ -meson decays. It may be noted that the CKM matrix elements and decay constants do not contribute to the ratio  $\mathcal{R}$ . The QCD parameter which appears in the decay amplitudes and the theoretical uncertainties caused by naive factorization for nonleptonic decays also get canceled a lot in calculating the observable  $\mathcal{R}$ . Contrary to other observables, the above mentioned ratios, in which the production of a  $B_c$  meson is canceled totally, provide an essential test of the decays. Besides giving useful information about the form factors, these ratios could offer a test of the adopted quark model. Our predicted observables ( $\mathcal{R}$ ) are listed in Table VIII. One can see that our results for the ratios  $\mathcal{R}_{K/\pi}$ ,  $\mathcal{R}_{D_s/\pi}$ , and  $\mathcal{R}_{\psi(2S)/J/\psi}$  are consistent with the LHCb data within experimental uncertainties. In particular, our predicted  $\mathcal{R}_{D_s/\pi} = 3.7832$  exactly matches the central value of the experimental data from the ATLAS Collaboration [15].

TABLE VIII. Ratios of branching fractions:  $\mathcal{R}$ .

Ratios $\mathcal{R}$	Our work	Experiment
$\mathcal{R}_{K/\pi} = \frac{\mathcal{B}(B_c \rightarrow J/\psi K)}{\mathcal{B}(B_c \rightarrow J/\psi \pi)}$	0.0783	$0.069 \pm 0.019(\text{Stat.}) \pm 0.005(\text{syst.})$
$\mathcal{R}_{D_s/\pi} = \frac{\mathcal{B}(B_c \rightarrow J/\psi D_s)}{\mathcal{B}(B_c \rightarrow J/\psi \pi)}$	3.7832	$0.079 \pm 0.007(\text{stat.}) \pm 0.003(\text{syst.})$
$\mathcal{R}_{\psi(2S)/J/\psi} = \frac{\mathcal{B}(B_c \rightarrow \psi(2S)\pi)}{\mathcal{B}(B_c \rightarrow J/\psi \pi)}$	0.3394	$0.250 \pm 0.068(\text{Stat.}) \pm 0.014(\text{Syst.}) \pm 0.006$
$\mathcal{R}_{\pi^+/\mu^+\nu} = \frac{\mathcal{B}(B_c \rightarrow J/\psi \pi)}{\mathcal{B}(B_c \rightarrow J/\psi \mu^+ \nu)}$	0.0142	$0.049 \pm 0.0028(\text{Stat.}) \pm 0.0046(\text{Syst.})$

Compared with the predictions of other theoretical studies, our predicted  $\mathcal{R}_{D_s/\pi}$  is found very close to  $3.45_{-0.17}^{+0.49}$  of Rui *et al.* [21] in their studies based on the PQCD approach and comparable to 2.6 (QCD PM) [27], 2.2 (BSW RQM) [59],  $2.06 \pm 0.86$  (LFQM) [22], 2.0 (RCQM) [38], 1.3 (QCD SR) [34], and  $1.29 \pm 0.26$  (CCQM) [38]. Only the predicted ratio  $\mathcal{R}_{\pi/\mu\nu}$  is found to be underestimated. Since the related ratios are mostly determined by the hadron transition, the agreement between the observed values and our predictions indicates a strong support to our approach to study nonleptonic  $B_c$  decays within the framework of the RIQ model.

## V. SUMMARY AND CONCLUSION

In this work, we study the exclusive two-body nonleptonic  $B_c \rightarrow X_{c\bar{c}}M$  decays, where  $X_{c\bar{c}}$  is a  $S$ -wave charmonium state and  $M$  is either a pseudoscalar ( $P$ ) or a vector ( $V$ ) meson. We consider here three categories of decays:  $B_c \rightarrow PP, PV, VP$  decays within the factorization approximation in the framework of the relativistic independent quark (RIQ) model based on a flavor-independent interaction potential in the scalar-vector harmonic form. The weak decay form factors representing decay amplitudes and their  $q^2$  dependence are extracted in the entire kinematic range of  $0 \leq q^2 \leq q_{\text{max}}^2$  from the overlapping integrals of the meson wave functions obtainable in the RIQ model.

In calculating the decay modes, we find our predicted branching fractions in a wide range  $\sim 10^{-2}$  to  $10^{-5}$ , in reasonable agreement with most other model predictions. The dominant decay modes to  $1S$  charmonium states are  $B_c^- \rightarrow \eta_c(\rho^-, D_s^-, D_s^{*-})$  and  $B_c \rightarrow J/\psi D_s^-$  which should be experimentally accessible. The branching fractions to  $2S$  and  $3S$  charmonium states  $B_c^- \rightarrow \eta'_c(\rho^-, D_s^-, D_s^{*-})$ ,  $B_c \rightarrow \psi' D_s^-$ , and  $B_c \rightarrow \eta''_c(\rho^-, D_s^-, D_s^{*-})$ ,  $B_c \rightarrow \psi'' D_s^-$  predicted up to  $\sim 10^{-4}$  may be accessible at high luminosity hadron colliders in near future. Other decay modes with lower branching fractions cannot reach the detection ability of current experiments. As expected, our predicted branching fractions are obtained in the hierarchy,

$$\begin{aligned} \mathcal{B}(B_c \rightarrow X_{c\bar{c}}(3S)M) &< \mathcal{B}(B_c \rightarrow X_{c\bar{c}}(2S)M) \\ &< \mathcal{R}(B_c \rightarrow X_{c\bar{c}}(1S)M). \end{aligned}$$

This is due to the nodal structure of the participating meson wave functions in the decays to higher excited states, tighter phase space, and weaker  $q^2$  dependence of the form factors for the decays to higher excited states in comparison to the decays to ground ( $1S$ ) states.

The class I decays determined by QCD coefficient  $a_1$  are found to have comparatively large branching fractions which should be measured experimentally. The class III decays, characterized by Pauli interference, are determined by both QCD parameters  $a_1$  and  $a_2$ . Considering the positive values of  $a_1$  and negative value of  $a_2$  used in the literature, this leads to destructive interference, as a result of which this class of decays is found to be suppressed compared to the case where the interference is switched off. We find the interference is more significant in class III  $B_c$  decays to higher excited  $2S$  and  $3S$  states compared to that found in the decays  $1S$  final states.

In the wake of recent measurements of the ratios of branching fractions by the LHCb Collaboration for nonleptonic  $B_c$  decays, these ratios are calculated in the present study, and our predicted ratios of branching fractions  $\mathcal{R}_{K/\pi}$ ,  $\mathcal{R}_{D_s/\pi}$ , and  $\mathcal{R}_{\psi(2S)/J/\psi}$  are consistent with the LHCb data within experimental uncertainties, although our prediction of  $\mathcal{R}_{\pi/\mu\nu}$  is found to be underestimated. Since the CKM parameters and decay constants do not contribute and the QCD parameter and the theoretical uncertainties due to naive factorization are also canceled a lot in calculating the ratio  $\mathcal{R}$ , these predicted ratios, contrary to other observables, could offer a test for the phenomenological models adopted in the description of nonleptonic decays. Our results for the weak form factors, branching fractions, and ratio  $\mathcal{R}$  indicate that the approach adopted here works well to describe nonleptonic  $B_c$  decays within factorization approximation in the framework of the RIQ model.

## APPENDIX: CONSTITUENT QUARK ORBITALS AND MOMENTUM PROBABILITY AMPLITUDES

In the RIQ model, a meson is pictured as a color-singlet assembly of a quark and an antiquark independently confined by an effective and average flavor-independent potential in the form  $U(r) = \frac{1}{2}(1 + \gamma^0)(ar^2 + V_0)$ , where  $(a, V_0)$  are the potential parameters. It is believed that the

zeroth order quark dynamics generated by the phenomenological confining potential  $U(r)$  taken in equally mixed scalar-vector harmonic form can provide an adequate tree-level description of the decay process being analyzed in this work. With the interaction potential  $U(r)$  put into the zeroth order quark Lagrangian density, the ensuing Dirac equation admits a static solution of positive and negative energy as

$$\begin{aligned}\psi_{\xi}^{(+)}(\vec{r}) &= \left( \frac{ig_{\xi}(r)}{r} \right) U_{\xi}(\hat{r}), \\ \psi_{\xi}^{(-)}(\vec{r}) &= \left( \frac{i(\vec{\sigma}\cdot\hat{r})f_{\xi}(r)}{r} \right) \tilde{U}_{\xi}(\hat{r}),\end{aligned}\quad (\text{A1})$$

where,  $\xi = (nlj)$  represents a set of Dirac quantum numbers specifying the eigenmodes, and  $U_{\xi}(\hat{r})$  and  $\tilde{U}_{\xi}(\hat{r})$  are the spin angular parts given by

$$\begin{aligned}U_{ljm}(\hat{r}) &= \sum_{m_l, m_s} \langle lm_l \frac{1}{2} m_s | jm \rangle Y_l^{m_l}(\hat{r}) \chi_{\frac{1}{2}}^{m_s}, \\ \tilde{U}_{ljm}(\hat{r}) &= (-1)^{j+m-l} U_{lj-m}(\hat{r}).\end{aligned}\quad (\text{A2})$$

With the quark binding energy  $E_q$  and quark mass  $m_q$  written in the form  $E'_q = (E_q - V_0/2)$ ,  $m'_q = (m_q + V_0/2)$ , and  $\omega_q = E'_q + m'_q$ , one can obtain solutions to the resulting radial equation for  $g_{\xi}(r)$  and  $f_{\xi}(r)$  in the form

$$\begin{aligned}g_{nl} &= N_{nl} \left( \frac{r}{r_{nl}} \right)^{l+1} \exp(-r^2/2r_{nl}^2) L_{n-1}^{l+1/2}(r^2/r_{nl}^2), \\ f_{nl} &= N_{nl} \left( \frac{r}{r_{nl}} \right)^l \exp(-r^2/2r_{nl}^2) \\ &\times \left[ \left( n + l - \frac{1}{2} \right) L_{n-1}^{l-1/2}(r^2/r_{nl}^2) + n L_n^{l-1/2}(r^2/r_{nl}^2) \right],\end{aligned}\quad (\text{A3})$$

where,  $r_{nl} = a\omega_q^{-1/4}$  is a state-independent length parameter, and  $N_{nl}$  is an overall normalization constant given by

$$N_{nl}^2 = \frac{4\Gamma(n)}{\Gamma(n+l+1/2)} \frac{(\omega_{nl}/r_{nl})}{(3E'_q + m'_q)},\quad (\text{A4})$$

and  $L_{n-1}^{l+1/2}(r^2/r_{nl}^2)$  etc. are associated Laguerre polynomials. The radial solutions yield an independent quark bound-state condition in the form of a cubic equation,

$$\sqrt{(\omega_q/a)}(E'_q - m'_q) = (4n + 2l - 1).\quad (\text{A5})$$

The solution of the cubic equation provides the zeroth order binding energies of the confined quark and antiquark for all possible eigenmodes.

In the relativistic independent particle picture of this model, the constituent quark and antiquark are thought to move independently inside the  $B_c$ -meson bound state with momenta  $\vec{p}_b$  and  $\vec{p}_c$ , respectively. Their individual momentum probability amplitudes are obtained in this model via momentum projection of respective quark orbitals (A1) in following forms:

For ground state mesons ( $n = 1, l = 0$ ),

$$\begin{aligned}G_b(\vec{p}_b) &= \frac{i\pi\mathcal{N}_b}{2\alpha_b\omega_b} \sqrt{\frac{(E_{p_b} + m_b)}{E_{p_b}}} (E_{p_b} + E_b) \exp\left(-\frac{\vec{p}_b^2}{4\alpha_b}\right), \\ \tilde{G}_c(\vec{p}_c) &= -\frac{i\pi\mathcal{N}_c}{2\alpha_c\omega_c} \sqrt{\frac{(E_{p_c} + m_c)}{E_{p_c}}} (E_{p_c} + E_c) \\ &\times \exp\left(-\frac{\vec{p}_c^2}{4\alpha_c}\right).\end{aligned}\quad (\text{A6})$$

For the excited meson state ( $n = 2, l = 0$ ),

$$\begin{aligned}G_b(\vec{p}_b) &= \frac{i\pi\mathcal{N}_b}{2\alpha_b} \sqrt{\frac{(E_{p_b} + m_b)}{E_{p_b}}} \frac{(E_{p_b} + E_b)}{(E_b + m_b)} \\ &\times \left( \frac{\vec{p}_b^2}{2\alpha_b} - \frac{3}{2} \right) \exp\left(-\frac{\vec{p}_b^2}{4\alpha_b}\right), \\ \tilde{G}_c(\vec{p}_c) &= \frac{i\pi\mathcal{N}_c}{2\alpha_c} \sqrt{\frac{(E_{p_c} + m_c)}{E_{p_c}}} \frac{(E_{p_c} + E_c)}{(E_c + m_c)} \\ &\times \left( \frac{\vec{p}_c^2}{2\alpha_c} - \frac{3}{2} \right) \exp\left(-\frac{\vec{p}_c^2}{4\alpha_c}\right).\end{aligned}\quad (\text{A7})$$

For the excited meson state ( $n = 3, l = 0$ ),

$$\begin{aligned}G_b(\vec{p}_b) &= \frac{i\pi\mathcal{N}_b}{2\alpha_b} \sqrt{\frac{(E_{p_b} + m_b)}{E_{p_b}}} \frac{(E_{p_b} + E_b)}{(E_b + m_b)} \\ &\times \left( \frac{\vec{p}_b^4}{8\alpha_b^2} - \frac{5\vec{p}_b^2}{4\alpha_b} + \frac{15}{8} \right) \exp\left(-\frac{\vec{p}_b^2}{4\alpha_b}\right), \\ \tilde{G}_c(\vec{p}_c) &= \frac{i\pi\mathcal{N}_c}{2\alpha_c} \sqrt{\frac{(E_{p_c} + m_c)}{E_{p_c}}} \frac{(E_{p_c} + E_c)}{(E_c + m_c)} \\ &\times \left( \frac{\vec{p}_c^4}{8\alpha_c^2} - \frac{5\vec{p}_c^2}{4\alpha_c} + \frac{15}{8} \right) \exp\left(-\frac{\vec{p}_c^2}{4\alpha_c}\right).\end{aligned}\quad (\text{A8})$$

The binding energies of constituent quarks and antiquarks for the ground state of  $B_c$  mesons as well as the ground and excited final meson states for  $n = 1, 2, 3; l = 0$  can also be obtained by solving respective cubic equations representing appropriate bound state conditions.

- [1] Particle Data Group, *Phys. Rev. D* **98**, 030001 (2018).
- [2] F. Abe *et al.* (CDF Collaboration), *Phys. Rev. D* **58**, 112004 (1998); *Phys. Rev. Lett.* **81**, 2432 (1998).
- [3] Belle Collaboration, *Phys. Rev. Lett.* **89**, 102001 (2002).
- [4] R. Aaij *et al.* (LHCb Collaboration), *Phys. Rev. Lett.* **108**, 251802 (2012).
- [5] R. Aaij *et al.* (LHCb Collaboration), *J. High Energy Phys.* **09** (2013) 075.
- [6] R. Aaij *et al.* (LHCb Collaboration), *Phys. Rev. D* **87**, 112012 (2013).
- [7] R. Aaij *et al.* (LHCb Collaboration), *J. High Energy Phys.* **11** (2013) 094.
- [8] R. Aaij *et al.* (LHCb Collaboration), *Phys. Rev. Lett.* **111**, 181801 (2013).
- [9] N. Brambilla *et al.* (Quarkonium Working Group), arXiv: hep-ph/0412158.
- [10] I. P. Gouz *et al.*, *Yad. Fiz.* **67**, 1581 (2004) [*Phys. At. Nucl.* **67**, 1559 (2004)].
- [11] S. Descotes-Genon, J. He, E. Kou, and P. Robbe, *Phys. Rev. D* **80**, 114031 (2009); C.-H. Chang and X.-G. Wu, *Eur. Phys. J. C* **38**, 267 (2004).
- [12] Y.-N. Gao, J.-B. He, R. Patrick, S. Marie-hélène, and Z.-W. Yang, *Chin. Phys. Lett.* **27**, 061302 (2010).
- [13] R. Aaij *et al.* (LHCb Collaboration), *J. High Energy Phys.* **09** (2013) 075.
- [14] R. Aaij *et al.* (LHCb Collaboration), *J. High Energy Phys.* **09** (2016) 153.
- [15] G. Aad *et al.* (ATLAS Collaboration), *Eur. Phys. J. C* **76**, 4 (2016).
- [16] R. Aaij *et al.* (LHCb Collaboration), *Phys. Rev. D* **87**, 071103 (2013).
- [17] R. Aaij *et al.* (LHCb Collaboration), *Phys. Rev. D* **90**, 032009 (2014).
- [18] X. Liu, Z.-J. Xiao, and C.-D. Lu, *Phys. Rev. D* **81**, 014022 (2010).
- [19] Z. Rui, H. Li, G.-x. Wang, and Y. Xiao, *Eur. Phys. J. C* **76**, 564 (2016).
- [20] Z. Rui, W. F. Wang, G. Wang, Li-hua Song, and C. D. Lü, *Eur. Phys. J. C* **75**, 293 (2015).
- [21] Z. Rui and Z. T. Zho, *Phys. Rev. D* **90**, 114030 (2014).
- [22] H. W. Ke, T. Liu, and X. Q. Li, *Phys. Rev. D* **89**, 017501 (2014).
- [23] I. Bediaga and J. H. Muñoz, arXiv:1102.2190v2.
- [24] D. Ebert, R. Faustov, and V. Galkin, *Phys. Rev. D* **68**, 094020 (2003).
- [25] J. F. Liu and K. T. Chao, *Phys. Rev. D* **56**, 4133 (1997).
- [26] C. H. Chang, H. F. Fu, G. L. Wang, and J. M. Zhang, *Sci. China Phys. Mech. Astron.* **58**, 071001 (2015).
- [27] P. Colangelo and F. De Fazio, *Phys. Rev. D* **61**, 034012 (2000).
- [28] H.-f. Fu, Y. Jiang, C. S. Kim, and G.-L. Wang, *J. High Energy Phys.* **06** (2011) 015.
- [29] T. Zhou, T. Anhong, Y. Jiang, L. Huo, and G.-L. Wang, arXiv:2006.05704v2.
- [30] T. Zhou, T. Wang, H. F. Fu, Z. H. Wang, L. Huo, and G. Li Wang, *Eur. Phys. J. C* **81**, 339 (2021).
- [31] E. Hernandez, J. Nieves, and J. M. Verde-Velasco, *Phys. Rev. D* **74**, 074008 (2006).
- [32] A. Y. Anisimov, I. M. Narodetsky, C. Semay, and B. Silvestre-Brac, *Phys. Lett. B* **452**, 129 (1999); A. Y. Anisimov, P. Y. Kulikov, I. M. Narodetsky, and K. A. Ter-Martirosian, *Yad. Fiz.* **62**, 1868 (1999).
- [33] A. Abd El-Hady, J. H. Munoz, and J. P. Vary, *Phys. Rev. D* **62**, 014019 (2000).
- [34] V. V. Kiselev, A. E. Kovalsky, and A. K. Likhoded, *Phys. At. Nucl.* **64**, 1860 (2001); *Nucl. Phys.* **B585**, 353 (2000); V. V. Kiselev, O. N. Pakhomova, and V. A. Saleev, *J. Phys. G* **28**, 595 (2002); V. V. Kiselev, arXiv:hep-ph/0211021; X. Q. Yu and X. L. Zhou, *Phys. Rev. D* **81**, 037501 (2010).
- [35] C. H. Chang and Y. Q. Chen, *Phys. Rev. D* **49**, 3399 (1994).
- [36] A. Issadykov and M. A. Ivanov, *Phys. Lett. B* **783**, 178 (2018).
- [37] S. Dubnika, A. Z. Dubnikov, A. Issadykov, M. A. Ivanov, and A. Liptaj, *Phys. Rev. D* **96**, 076017 (2017).
- [38] M. A. Ivanov, J. G. Korner, and P. Santorelli, *Phys. Rev. D* **73**, 054024 (2006).
- [39] N. Barik and B. K. Dash, *Phys. Rev. D* **33**, 1925 (1986); N. Barik, B. K. Dash, and P. C. Dash, *Pramana J. Phys.* **29**, 543 (1987); N. Barik and P. C. Dash, *Phys. Rev. D* **47**, 2788 (1993).
- [40] N. Barik, P. C. Dash, and A. R. Panda, *Phys. Rev. D* **46**, 3856 (1992); N. Barik and P. C. Dash, *Phys. Rev. D* **49**, 299 (1994); M. Priyadarsini, P. C. Dash, S. Kar, S. P. Patra, and N. Barik, *Phys. Rev. D* **94**, 113011 (2016); N. Barik and P. C. Dash, *Mod. Phys. Lett. A* **10**, 103 (1995); N. Barik, S. Kar, and P. C. Dash, *Phys. Rev. D* **57**, 405 (1998); N. Barik, Sk. Naimuddin, S. Kar, and P. C. Dash, *Phys. Rev. D* **63**, 014024 (2000).
- [41] N. Barik, P. C. Dash, and A. R. Panda, *Phys. Rev. D* **47**, 1001 (1993); N. Barik and P. C. Dash, *Phys. Rev. D* **47**, 2788 (1993); N. Barik, Sk. Naimuddin, P. C. Dash, and S. Kar, *Phys. Rev. D* **77**, 014038 (2008); N. Barik, Sk. Naimuddin, P. C. Dash, and S. Kar, *Phys. Rev. D* **78**, 114030 (2008); N. Barik, Sk. Naimuddin, and P. C. Dash, *Int. J. Mod. Phys. A* **24**, 2335 (2009).
- [42] N. Barik and P. C. Dash, *Phys. Rev. D* **53**, 1366 (1996); N. Barik, S. K. Tripathy, S. Kar, and P. C. Dash, *Phys. Rev. D* **56**, 4238 (1997); N. Barik, Sk. Naimuddin, P. C. Dash, and S. Kar, *Phys. Rev. D* **80**, 074005 (2009).
- [43] S. Patnaik, P. C. Dash, S. Kar, S. P. Patra, and N. Barik, *Phys. Rev. D* **96**, 116010 (2017); S. Patnaik, P. C. Dash, S. Kar, and N. Barik, *Phys. Rev. D* **97**, 056025 (2018).
- [44] S. Patnaik, L. Nayak, P. C. Dash, S. Kar, and N. Barik, *Eur. Phys. J. Plus* **135**, 936 (2020).
- [45] L. Nayak, S. Patnaik, P. C. Dash, S. Kar, and N. Barik, *Phys. Rev. D* **104**, 036012 (2021).
- [46] N. Barik, S. Kar, and P. C. Dash, *Phys. Rev. D* **63**, 114002 (2001); N. Barik, Sk. Naimuddin, P. C. Dash, and S. Kar, *Phys. Rev. D* **80**, 014004 (2009).
- [47] S. Naimuddin, S. Kar, M. Priyadarshini, N. Barik, and P. C. Dash, *Phys. Rev. D* **86**, 094028 (2012); S. Kar, P. Dash, M. Priyadarsini, Sk. Naimuddin, and N. Barik, *Phys. Rev. D* **88**, 094014 (2013).
- [48] M. Wirbel, B. Stech, and M. Bauer, *Z. Phys. C* **29**, 637 (1985); M. Bauer, B. Stech, and M. Wirbel, *Z. Phys. C* **34**, 103 (1987); L.-L. Chau, H.-Y. Cheng, W. K. Sze, H. Yao, and B. Tseng, *Phys. Rev. D* **43**, 2176 (1991); **58**, 019902 (1998).

- [49] I. P. Gouz, V. V. Kiselev, A. K. Likhoded, V. I. Romanovsky, and O. P. Yushchenko, *Phys. At. Nucl.* **67**, 1559 (2004).
- [50] M. Beneka, G. Buchalla, M. Neubert, and C. T. Sachrajda, *Phys. Rev. Lett.* **83**, 1914 (1999); *Nucl. Phys.* **B591**, 313 (2000); **B606**, 245 (2001); M. Beneka and M. Neubert, *Nucl. Phys.* **B675**, 33 (2003); C. E. Thomas, *Phys. Rev. D* **73**, 054016 (2006).
- [51] J. D. Bjorken, in *Proceedings of the International Workshop, Crete, Greece, 1988*, edited by G. Branco and J. Reeo, Development in High Energy Physics [Nucl. Phys. B Proc. Suppl. 11, 325 (1989)].
- [52] A. J. Buras, J. M. Gerard, and R. Ruckl, *Nucl. Phys.* **B268**, 16 (1986).
- [53] M. Neubert, *Phys. Rep.* **245**, 259 (1994).
- [54] M. Neubert and B. Stech, *Adv. Ser. Dir. High Energy Phys.* **17**, 294 (1998).
- [55] H. M. Choi and C. R. Ji, *Phys. Rev. D* **80**, 114003 (2009).
- [56] J. Sun, D. Du, and Y. Yang, *Eur. Phys. J. C* **60**, 107 (2009); J. Sun, Y. Yang, W. Du, and H. Ma, *Phys. Rev. D* **77**, 114004 (2008); J. Sun, G. Xue, Y. Yang, G. Lu, and D. Du, *Phys. Rev. D* **77**, 074013 (2008).
- [57] C. E. Thomas, *Phys. Rev. D* **73**, 054016 (2006).
- [58] G. Buchalla *et al.*, *Eur. Phys. J. C* **57**, 309 (2008); A. J. Buras, [arXiv:hep-ph/9806471](https://arxiv.org/abs/hep-ph/9806471).
- [59] N. Sharma and R. C. Verma, *Phys. Rev. D* **82**, 094014 (2010); N. Sharma, R. Dhir, and R. C. Verma, *J. Phys. G* **37**, 075013 (2010); R. Dhir and R. C. Verma, *Phys. Rev. D* **79**, 034004 (2009); N. Sharma, *Phys. Rev. D* **81**, 014027 (2010).
- [60] B. Margolis and R. R. Mendel, *Phys. Rev. D* **28**, 468 (1983).
- [61] P. Zyla *et al.* (Particle Data Group), *Prog. Ther. Exp. Phys.* **2020**, 083C01 (2020).
- [62] P. Abreu *et al.* (DELPHI Collaboration), *Phys. Lett. B* **426**, 231 (1998).
- [63] R. Aaij *et al.* (LHCb Collaboration), *J. High Energy Phys.* **02** (2016) 133.
- [64] S. Godfrey and K. Moats, *Phys. Rev. D* **93**, 034035 (2016).
- [65] H. Wang, Z. Yan, and J. Ping, *Eur. Phys. J. C* **75**, 196 (2015).
- [66] W. Lucha, D. Melikhov, and S. Simula, *Phys. Lett. B* **735**, 12 (2014).
- [67] D. Becirevic, G. Duplancic, B. Klajn, B. Melic, and F. Sanfilippo, *Nucl. Phys.* **B883**, 306 (2014).
- [68] T. E. Browder and K. Honscheid, *Prog. Part. Nucl. Phys.* **35**, 81 (1995); M. Neubert, V. Rieckert, B. Stech, and Q. P. Xu, in *Heavy Flavors*, edited by A. J. Buras and H. Lindner (World Scientific, Singapore, 1992) and references therein.
- [69] L. Wolfenstein, *Phys. Rev. Lett.* **51**, 1945 (1983).